

Role of Prostaglandin in Mediastinal Lymph Node Metastasis

and Pre-metastatic Niche Formation in Lung Cancer

(肺癌リンパ節転移および premetastatic niche 形成におけるプロスタグランジンの役割)

氏 名 小川 史洋

【背景・目的】

原発性肺癌は全世界において死亡者数が増加しており、難治癌とされている悪性腫瘍の一つである。この死亡者数増加は、早期に所属リンパ節や他臓器への血行性・リンパ行性転移をすることが原因の一つとしてあげられる。血行性転移については血管新生等の研究において解明されつつあるが、リンパ節転移に関してはそのメカニズムの解明が遅れている。現在、腫瘍発育や血管新生において Cyclooxygenase (COX)-2 や Prostaglandin (PG) が深く関与していると報告されているが、リンパ管新生・リンパ節転移へのこれらの関与についてはまだ明らかにされていない。そこで、肺癌の所属リンパ節転移に注目し、肺癌リンパ節転移のマウスモデルを作成した上で COX-PGs の関連・それらに關与する微小循環における Cytokine (SDF-1/CXCR4, TGF- β など) や免疫担当細胞 (Dendritic cells, regulatory T cells など) の構成因子を解析し、リンパ節転移メカニズムについて解析することを立案した。

【材料・方法】

C56BL6 マウスを用い、Lewis Lung Carcinoma (LLC; $5 \times 10^4/10 \mu\text{L}$) 細胞を Matrigel® と混合し、左肺に直接移植することで肺癌リンパ節転移モデルを作成した。COX/ COX-2、SDF-1/CXCR4、PGE₂/EP3 signaling との関連を解明するため、COX inhibitor (aspirin)、COX-2 inhibitor (celecoxib)、SDF-1 antagonist (AMD3100) の経口投与、EP3KO マウスを用いて同実験を行った。

さらに、Dendritic cells (DCs) や regulatory T cells (Tregs) がいかに関与しているかを co-cultured DCs と PGE₂ agonist、各種 EP agonist を用いて解析した。

【結果】

肺癌リンパ節転移モデルは腫瘍移植後 10-12 日目に再現性をもって作成可能であった。COX/ COX-2 inhibitor 投与群においてリンパ節転移の抑制が確認され、リンパ節内 subcapsular sinus における前転移状態 (pre-metastatic phase) での SDF-1 発現の低下が確認された。さらに SDF-1 antagonist を用いた実験でも、リンパ節転移の抑制を確認し、SDF-1 が COX-2/PGE₂ signaling により pre-metastatic niche formation の形成に関与していると考えた。PG receptor

で EP3 がリンパ節転移にもっとも関与していると判明したため、EP3KO マウスを用いるとリンパ節転移の抑制が認められた。ここで DCs, Tregs のリンパ節転移への関与を確認すると、vehicle 群に比べるとリンパ節内 subcapsular sinus での発現が有意に低下していた。

実際野生株と EP3KO マウスからそれぞれ骨髄細胞から co-culture した DCs を骨髄移植し、腫瘍の転移の具合を確認すると、EP3KO DCs 移植群で有意なリンパ節転移の抑制が認められた。また、この DCs に PGE₂ antagonist, EP3 agonist を添付すると SDF-1/TGF- β の分泌の亢進が確認され、これが pre-metastatic niche formation, リンパ節転移に関与していると考えられた。

【結語】

縦隔リンパ節における pre-metastatic niche formation は COX-2 誘導性 PGE₂-EP3 signaling, SDF-1/CXCR4, TGF- β による DCs や Tregs の骨髄からの動員により引き起こされると考えられた。それゆえ、COX-2 inhibitor や CXCR4 antagonist, EP3 antagonist や DCs を介した免疫療法が今後の肺癌治療の一つの選択肢になり得、予後改善の可能性はある。

学位論文

「Role of Prostaglandin in Mediastinal Lymph Node Metastasis
and Pre-metastatic Niche Formation in Lung Cancer」

(肺癌リンパ節転移および premetastatic niche 形成におけるプロ
スタグランジンの役割)

DM10011 小川 史洋

北里大学大学院医療系研究科医学専攻博士課程
分子病態学群 分子薬理学
指導教授 馬嶋 正隆

著者の宣言

本学位論文は、著者の責任において実験を遂行し、得られた真実の結果に基づいて正確に作成したものに相違ないことをここに宣言する。

論文要旨

【背景・目的】

原発性肺癌は全世界において死亡者数が多く、予後が悪いとされている悪性腫瘍の一つである。この死亡者数の多さは、早期に所属リンパ節や他臓器への血行性・リンパ行性転移をすることが原因の一つとしてあげられる。血行性転移については血管新生等々の研究において解明されつつあるが、リンパ節転移に関してはまだ解明が乏しいところである。現在、腫瘍発育や血管新生において Cyclooxygenase (COX)-2 や Prostaglandin (PGs) が関与していると報告されているが、リンパ管新生・リンパ節転移への関与についてはまだ明らかにされていない。このリンパ節転移を解明することにより肺癌の予後改善が見込まれると考え、今回の実験を行うこととした。COX-2 誘導性 PGE₂ が肺癌リンパ節転移にどのように影響しているか。またいかなる腫瘍周囲微小環境構成因子（サイトカインや免疫担当細胞など）がリンパ節転移に関与しているかの検討を行った。

【材料・方法】

C56BL6 マウスを用い、Lewis Lung Carcinoma (LLC; $5 \times 10^4/10 \mu\text{L}$) 細胞を Matrigel® と混合し、左肺に直接移植することで肺癌リンパ節転移モデルを作成した。COX/COX-2、SDF-1/CXCR4, PGE₂/EP3 signaling との関連を解明するため、COX inhibitor (aspirin), COX-2 inhibitor (celecoxib)、SDF-1 antagonist (AMD3100) の経口投与、EP3KO マウスを用いて同実験を行った。

さらに、Dendritic cells (DCs) や regulatory T cell (Treg) がいかに関与しているかを co-cultured DCs と PGE₂ agonist, 各種 EP agonist を用いて解析した。

【結果】

肺癌リンパ節転移モデルは腫瘍移植後 10-12 日目に再現性をもって作成可能であった。COX/COX-2 inhibitor 投与群においてリンパ節転移の抑制が確認され、リンパ節内 subcapsular sinus における前転移状態 (premetastatic phase) での SDF-1 発現の低下が確認された。さらに SDF-1 antagonist を用いた実験でも、リンパ節転移の抑制を確認し、SDF-1 が COX-2/PGE₂ signaling により premetastatic niche formation の形成に関与していると考えた。PG receptor で EP3 がリンパ節転移にもっとも関与していると判明したため、EP3KO マウスを用いるとリンパ節転移の抑制が認められた。ここで DCs, Treg のリンパ節転移への関与を確認すると、vehicle 群に比べるとリンパ節内 subcapsular sinus での発現が有意に低下していた。

実際野生株と EP3KO マウスからそれぞれ骨髓細胞から co-culture した DCs を骨髓移植し、腫瘍の転移の具合を確認すると、EP3KO DCs 移植群で有意なリンパ節転移の抑制が認められた。また、この DCs に PGE₂ agonist, EP3 agonist を添付すると SDF-1/TGF- β の分泌の亢進が確認され、これが premetastatic niche formation, リンパ節転移に関与していると考えられた。

【結語】

縦隔リンパ節における premetastatic niche formation は COX-2 誘導性 PGE₂-EP3 signaling, SDF-1/CXCR4, TGF- β による DCs や Treg の骨髓からの動員により引き起こされると考えられた。それゆえ、COX-2 inhibitor や CXCR4 antagonist, EP3 antagonist や DCs を介した免疫療法が今後の肺癌治療の一つの選択肢になり得、祖語改善の可能性がある。

目次

	頁
1. Abstract	1
2. Introduction	2
3. Material and Methods	4
3-1. Cell lines	4
3-2. Retroviral transfection of the GFP gene	4
3-3. Animals	4
3-4. Intrapulmonary implantation	4
3-5. Drugs	5
3-6. Evaluation of tumor size and lymph node metastasis	5
3-7. Fluorescence microscopy	5
3-8. Immunofluorescence	5
3-9. Calculation of %total cell population	6
3-10. Quantitative real time RT-PCR analysis	6
3-11. Bone marrow transplantation	6
3-12. BM-derived dendritic cells and cell culture	7
3-13. In vitro SDF-1 and TGFβ1 expression	7
3-14. Statistical Analysis	7
4. Results	
4-1. Survival rate of mice injected with LLC cells plus BD Matrigel	8
4-2. Time course of regional lymph node metastasis after the injection of ---- LLC-GFP cells plus BD Matrigel	8
4-3. Aspirin treatment reduces regional lymph node metastasis	8
4-4. Early expression of COX-2 in premetastatic regional lymph nodes and -- COX-2-derived PGE ₂ -EP3 signaling enhances lymph node metastasis	9
4-5. COX-2-dependent premetastatic niche formation in regional lymph ---- Nodes	9
4-6. The SDF-1/CXCR4 axis governs the accumulation of LLC cells in the --- lymph node premetastatic niche	10
4-7. COX-2-positive DCs accumulate in the lymph node premetastatic niche- and produce SDF-1 via EP3 signaling	10
4-8. EP3 signaling facilitates DCs recruitment to the regional lymph node ---- premetastatic niche	11
4-9. Both COX-2/EP3 signaling and SDF-1 increase the recruitment of ---- Tregs to the lymph node premetastatic niche	11
4-10. PGE ₂ -EP3 signaling as a regulator of lymph node lymphangiogenesis -	12
5. Discussion	13
6. Conclusion	15
7. Prospective	15
8. References	16

9. Figure legends	
9-1. Figure 1. Regional lymph node metastasis model. -----	21
9-2. Figure 2. Time course of regional lymph node metastasis ----- after the injection of LLC plus Matrigel.	21
9-3. Figure 3. Effect of aspirin on regional lymph node metastasis. -----	21
9-4. Figure 4. Effect of aspirin on GFP-positive LLC cell growth ----- and the expression of GFP in the regional lymph nodes.	22
9-5. Figure 5. COX-2 induction in regional lymph nodes and the effect ---- of COX-2 inhibition on regional lymph node metastasis	22
9-6. Figure 6. COX-2/EP3 enhances SDF-1 expression in lymph nodes ----	23
9-7. Figure 7. Effect of the SDF-1/CXCR4 axis on lymph node metastasis -	24
9-8. Figure 8. COX-2 derived PGE ₂ -EP3 signaling induces lymph node ---- metastasis and lymphangiogenesis by facilitating DCs recruitment	25
9-9. Figure 9. COX-2 derived PGE ₂ -EP3 signaling induces lymph node ----- metastasis by facilitating the accumulation of Treg cells	25
9-10. Figure 10. COX-2 derived PGE ₂ -EP3 signaling induces ----- lymphangiogenesis.	26
10. Figures -----	27
11. Supplement figures	
11-1. Figure S1. COX-2 inhibitor treatment does not affect the progression-- of the primary tumor in the early phase before regional lymph node metastasis.	37
11-2. Figure S2. SDF-1 induction in regional lymph nodes is essential for --- premetastatic niche formation.	38
11-3. Figure S3. Effect of PGE ₂ and EP agonists on the expression and ---- secretion of SDF-1 in cultured DCs.	39
11-4. Figure S4. Regulation of Tregs induction by COX-2 derived ----- PGE ₂ -EP3 signaling and effect on tumor metastasis	40
12. Acknowledgement -----	41

1. Abstract

Lung cancer is the main cause of cancer-related death worldwide. The high mortality is probably attributable to early metastasis; however, the mechanism underlying metastasis to regional lymph nodes is still unknown.

Lymphatic systems serve as an important route for spread of cancers, and lymph node metastasis (LNM) is a critical prognostic factor in cancer patients. We investigated roles of Cyclooxygenase (COX), especially one of the isozyme COX-2, derived prostaglandin (PG)E₂ in the formation of the premetastatic niche and LNM. COX- PGE₂ induces tumor growth and metastasis and is associated with a poor prognosis. So, we investigated the effect of an authentic COX inhibitor, aspirin, on regional lymph node metastasis during the development of lung cancer in mice in the present study.

Furthermore, COX-2 was expressed in the dendritic cells (DCs) from the early stage in the LN subcapsular sinus and COX-2 inhibition significantly suppressed mediastinal LNM, after injections of Lewis lung carcinoma (LLC) cells into the lungs. Stromal cell-derived factor(SDF)-1 expression elevated in DCs before LLC cell infiltration, was reduced with a COX-2 inhibitor, SDF-1 antagonist, and a CXCR4 neutralizing antibody. The same was true in EP3 knockout (KO) mice. Stimulation with an EP3 agonist increased production of SDF-1 in cultured DCs, and injection of EP3KO CD11c⁺DC cells significantly reduced the accumulation of SDF1⁺CD11c⁺DCs in regional lymph nodes and LNM compared with that in WT CD11c⁺DCs. Accumulation of regulatory T cells and lymph node lymphangiogenesis, both of which may decide the fate of metastasized tumor cells were also COX-2/EP3-dependent. These results indicate that DCs induce premetastatic niche formation during LNM via COX-2/EP3-dependent induction of SDF-1, and suggest that inhibitors of this mechanistic avenue are effective in suppressing premetastatic niche formation and LNM.

Key words: lung cancer; lymph node metastasis; COX-2; PGE₂; SDF-1; Dendritic cells

2. Introduction

Lung cancer is the most common cause of cancer mortality worldwide and non-small-cell lung cancer (NSCLC) accounts for 75–85% of all diagnosed lung cancers. Despite progress in surgical techniques, chemotherapy, and radiotherapy, the 5-year survival rate for patients with lung cancer is only 16%.¹ It is estimated that 226,160 new cases will be diagnosed in 2012 and 160,340 will die from the disease.² More than half of patients (56%) with lung cancer have either advanced or metastatic disease at the time of diagnosis and, even with chemotherapy, the median survival is 1 year or less.^{3, 4} Tumor recurrence and metastasis are the major causes of treatment failure and death. Metastasis a complex multistep process during which cells must acquire several distinct properties: loss of cell-to-cell adhesion and increased invasiveness, intravasation, and increased survival and proliferation are all prerequisites for the establishment of distant macrometastases.⁵⁻⁷ Despite progress in other areas of cancer therapeutics, the complexities of the process mean that cancer metastasis is still poorly understood. And, it is widely accepted that many tumors tend to metastasize to specific organs⁸. The mechanisms that guide tumor cells to specific tissues are largely unknown, although recent evidence suggests that it may involve molecular differences inherent in the tumor cells themselves, modulated by the activities of immune cells, hematopoietic cells, and other tissue components. Lymph node metastasis (LNM) is a critical prognostic factor in cancer patients, and lymphatic vessels serve as an important route for the spread of cancer cells⁸. Paget reported that tumor cells might prepare the lymph nodes for their future arrival, giving a new interpretation to the seed-and-soil hypothesis⁹. The formation of a premetastatic niche, suitable for the arrival of the first tumor cells, facilitates metastasis via the blood stream^{10, 11}. However, data regarding the factors involved in lymph node premetastatic niche formation are limited¹². Tumor-associated lymphangiogenesis may enhance metastasis to the regional lymph nodes; however, the involvement of lymph node premetastatic niche formation in the metastatic process is unclear.

In contrast, prostanoids, including prostaglandins (PGs), are generated from arachidonic acid via cyclooxygenase (COX) and specific PG synthases. These are the rate-limiting enzymes that regulate PG biosynthesis in various tissues.¹³⁻¹⁹ COX-2, an isoform of COX, is expressed at sites of inflammation and malignancy. We reported previously that COX-2 and receptor signaling by prostaglandins play crucial roles in lymphangiogenesis during chronic inflammation, secondary lymphedema, and tumor development.¹³⁻¹⁹ More precise understanding of the mechanisms underlying lymph node metastases, together with identification of the molecules involved, will improve the prognosis of lung cancer patients. Previous studies show that mice treated with COX inhibitors are resistant to the development of colorectal neoplasia, suggesting that COX inhibitors may be good therapeutic options.²⁰ The same may be true for humans; epidemiological studies show that non-steroidal anti-inflammatory drugs (NSAIDs), such as aspirin, a classical and authentic COX inhibitor, reduces the risk of developing several types of cancer.²¹ However, the precise role played by COX in

regional lymph node metastasis is not clear. The cellular components involved in tumor cells metastasis to a predetermined location are largely unknown. However, Kaplan et al.¹¹ demonstrated that bone marrow (BM)-derived hematopoietic progenitor cells expressing vascular endothelial growth factor receptor 1 (VEGFR1; also known as Flt1), home to tumor-specific premetastatic sites and form cellular clusters before the arrival of tumor cells. Their findings demonstrated a requirement for VEGFR1+ hematopoietic progenitors in the regulation of metastasis, and suggested that expression patterns of fibronectin and VEGFR1+VLA-4 (also known as integrin $\alpha 4\beta 1$)+ clusters dictate organ-specific tumor spread. However, the involvement of other cellular components in premetastatic niche formation is largely unknown. Among the many cellular components within the tumor microenvironment, dendritic cells (DCs) exert profound effects on T cells²². The mediators that regulate DCs function may also modulate niche formation. PGE₂ and the tryptophan catabolizing enzyme, indoleamine 2, 3-dioxygenase (IDO), exert strong effects on the maturation and function of DCs²³. In addition, PGE₂ has been identified as a major immunosuppressive soluble factor present in the tumor microenvironment^{24, 25}. An important mechanism by which these DCs modulate T cell responses seems to be via PGE₂-induced expression of IDO. Furthermore, a recent study reported that PGE₂ increased the immunosuppressive potential of regulatory T cells (Tregs)²⁶. We previously reported that COX and COX-2-derived endogenous PGE₂ enhanced angiogenesis and lymphangiogenesis during tumor development and chronic inflammation^{14, 15}. Furthermore, PGE₂ enhances stromal tissue formation and tumor-associated angiogenesis mediated by tumor stromal chemokines¹⁷. The function of a broad range of immune cells can be regulated by PGE₂; however, the precise contributions of PGE₂ to LNM are not clear.

In this study, we examined regional lymph node metastasis in a mouse model of lung cancer development and showed that endogenous COX-2-derived PGE₂ stimulated the EP3 receptor on DCs and up-regulated the expression of stromal cell derived factor-1 (SDF-1) in the subcapsular regions of regional lymph nodes following LLC cells injection. SDF-1 up-regulation increased the accumulation of CXCR4⁺ LLC cells and facilitated the formation of regional lymph node premetastatic niches. The accumulation of Tregs and lymph node lymphangiogenesis, both of which may influence the fate of metastasized tumor cells, were also COX-2/EP3-dependent. Thus, inhibitors of PGE₂, together with SDF-1 receptor antagonists and EP3 antagonists, may be effective at suppressing premetastatic niche formation and LNM. These findings strongly suggested a novel function of PGE₂ in the formation of the lymph node premetastatic niche.

3. Materials and Methods

3-1. Cell lines

LLC cells, originally isolated from C57Bl/6 mice, were cultured at 37°C in Dulbecco's modified Eagle's medium (DMEM; Gibco by Life Technologies, Grand Island, NY) supplemented with 10% fetal bovine serum (FBS; Gibco by Life Technologies, Grand Island, NY) in a humidified atmosphere containing 5% CO₂. LLC cells were purchased from Riken Brc Cell Bank (RBRV-RCB2638; Tsukuba, Japan).

3-2. Retroviral transfection of the GFP gene

Murine GFP cDNA was cloned into a deficient retroviral vector, pLEGFP (Clontech by Takara, Tokyo, Japan), and then transfected into PT67 cells (Clontech by Takara, Tokyo, Japan). The cells were then selected by culture with G418 (Roche, Basel, Schweiz). The resulting temporarily infectious recombinant GFP-containing virus was used to infect NIH/3T3 cells, which were then selected with G418 to evaluate the infectious titer. The titer was approximately 1×10^3 cfu/ml. LLC-GFP cells were infected with the temporarily infectious retroviruses and selected with G418. The selected cells were designed as LLC-GFP.

3-3. Animals

Male C57BL/6 mice, 6 to 8 weeks-old and weighing 20 to 25 g, were obtained from the CLEA Japan (Tokyo, Japan). EP3 receptor knockout mice (EP3 KO) on a C57BL/6 hybrid background were generated by our research group. The mice (male, 8 weeks old) were maintained at a constant humidity ($60 \pm 5\%$) and temperature ($20 \pm 1^\circ\text{C}$) and were kept continuously on a 12-hour light/ dark cycle. All animals were provided with food and water *ad libitum*. All experiments were performed in accordance with the guidelines for animal experiments of Kitasato University School of Medicine.

3-4. Intrapulmonary implantation

LLC-GFP cells (growing in log phase) were suspended in PBS (10 μl ; final cell density, $5 \times 10^4/\text{ml}$) containing 10 μl of BD Matrigel[®] (Becton Dickinson Labware, MA, USA) to prevent air leakage and hemothorax when injected into the lung. The cells were injected into the left lung parenchyma of mice anesthetized with ether¹⁷. A small skin incision (approximately 5 mm in length) was made in the chest wall in the left lateral thoracic region. While observing the motion of the left lung through the pleura, a 31 gauge needle attached to a 0.3 ml insulin syringe was directly inserted through the intercostal space into the lung (to a depth of 2–3 mm). After injecting the LLC cells, the skin incision was closed with a surgical suture.

3-5. Drugs

For the experiment to evaluate the inhibitory effect of NSAIDs, mice were orally administered aspirin (100 mg/kg, — 4 — Sigma-Aldrich, STL, USA) from Day 0 after LLC-GFP injection. A COX-2 inhibitor, celecoxib (100 mg/kg per day; Pfyser, Osaka, Japan) and a CXCR4 antagonist, AMD3100 (10 mg/kg per day; Sigma-Aldrich, St Louis, MO, USA) were administered orally every day. A CXCR4 neutralizing antibody (10 mg/mouse; clone 2B11; BD Biosciences, San Jose, CA) was injected intraperitoneally daily.

3-6. Evaluation of tumor size and lymph node metastasis

Mice were sacrificed at various time points after LLC-GFP cell injection, using ether, and the lungs were resected and the long and short diameters of the primary tumor masses were measured manually. The tumor volume was calculated using ImageJ software (NIH, MD, USA). Lungs harboring a primary tumor nodule and the mediastinal lymph nodes were excised for histological examination and fluorescence microscopy. The isolated lungs were fixed with 4% Paraformaldehyde (PFA) or 10% Formalin, and analyzed under a microscope.

3-7. Fluorescence microscopy

Mice were sacrificed as described above, and we observed the status of mediastinal lymph node metastasis examined under a fluorescence microscope (VHX-1000, KEYENCE, Osaka, Japan). The arbitrary units of fluorescence intensity were analyzed using VHX-1000 software (KEYENCE) and were compared between the vehicle-treated group and drug-treated or knockout group.

3-8. Immunofluorescence

For immunofluorescence cytochemistry, lung tissues were immediately fixed with 4% paraformaldehyde in 0.1 mol/L phosphate buffer solution (pH 7.4). After fixation, the tissues were dehydrated with graded ethanol series and then embedded in paraffin. Sections of the paraffin-embedded tissues (4 mm thick) were mounted on glass slides, deparaffinized with xylene, and placed in 4°C acetone. The sections were blocked with 1% bovine serum albumin-PBS and incubated with goat anti-mouse VEGF-C (1:200; Santa Cruz Biotechnology), goat anti-mouse VEGF-D (1:200; Santa Cruz Biotechnology), rabbit anti-mouse VEGFR-3 (1:200; Santa Cruz Biotechnology), goat anti-mouse COX-2 (1:500; Abcam), rat anti-mouse Stroma derived factor-1 (SDF-1) (1:50; Santa Cruz Biotechnology), C-X-C receptor type 4 (CXCR4) (1:50; BD Pharmingen), rabbit anti-mouse indoleamine 2, 3-dioxygenase (IDO) (1:200; Santa Cruz Biotechnology), ArHm anti-mouse CD11c (1:200; Abcam), and rat anti-mouse Foxp3 (1:500; eBioscience) antibodies. After washing in PBS, the sections were incubated with Alexa Fluor 488 goat anti-rabbit IgG (1:200; Invitrogen; Life Technologies, Carlsbad, CA) and Alexa Fluor 568 goat anti-rat IgG (1:200; Invitrogen; Life Technologies) or incubated with Universal DAKO LSABTM+ system-HRP (DAKO, North America, CA, USA) with DAB and Mayer's hematoxylin

solution.. Negative control staining was performed by replacing the primary antibodies with 1% bovine serum albumin-PBS. Images were captured with a confocal scanning laser microscope (LSM710; Carl Zeiss, Jena, Germany) or a microscope (BX51; Olympus, Japan).

3-9. Calculation of %total cell population

The ratio of immunohistochemistry positive cells for each antibody per field required for each point varies with the size of the high power field (HPF; $\times 400$) for a given microscope at regional lymph node by image J software.

3-10. Quantitative real time RT-PCR analysis

The excised tissue samples were immediately immersed in RNeasy Lysis Reagent (QIAGEN Japan, Tokyo, Japan), and homogenized for 60 seconds at 6000 rpm using a MagNALyser (Roche diagnostics Inc., Mannheim, Germany). Harvested cells were washed three times with PBS solution and homogenized using a QIA Shredder (QIAGEN Japan, Tokyo, Japan). Total RNA was extracted from the homogenized tissues and cells using the RNeasy Mini Kit (QIAGEN Japan, Tokyo, Japan), and single-stranded cDNA was generated from 1 μ g of total RNA via reverse transcription using ReverTra Ace (TOYOBO Co., Ltd., Osaka, Japan), according to the manufacturer's instructions. Quantitative PCR amplification was performed using SYBR Premix Ex Taq (Takara Bio Inc., Shiga, Japan). The real time RT-PCR primers for COX-2, TGF β , SDF-1, VEGF-C, VEGF-D, and VEGFR-3 were designed using Primer 3 software (<http://primer3.sourceforge.net>) based on data obtained from GenBank. The following primers were used for real-time RT-PCR: GAPDH forward, 5'-ACATCAAGAAGGTGGTGAAGC-3', and reverse, 5'-AAGGTGGAAGAGTGGGAGTTG-3'; GFP sense, 5'-ACTACAACAGCCACAACGTCT-3' and antisense, 5'-GGTGTCTGCTGGTAGTGGTC-3'; COX-2 sense, 5'-TGGGTGTGAAGGGAATAAGG-3' and antisense, 5'-CATCATATTTGAGCCTTGGGG-3'; SDF-1 sense, 5'-CAGAGCCAACGTCAAGCA-3' and antisense, 5'-AGGTACTCTTGGATCCAC-3'; TGF- β sense, 5'-AACAATTCCTGGCGTTACCTT-3' and antisense, 5'-TGTATTCCGTCTCCTTGGTTC-3'; VEGF-C sense, 5'-TCTGTGTCCAGCGTAGATGAG-3' and antisense, 5'-CATCATATTTGAGCCTTGGGG-3'; VEGF-D sense, 5'-CCTATTGACATGCTGTGGGAT-3' and antisense, 5'-GTGGGTTCCCTGGAGGTAAGAG-3'; and VEGFR-3 sense, 5'-TTTATGTCCCACCCCACTAC-3' and antisense, 5'-GGCTGAGCTACAAGGGCAATCG-3' (Sigma-Aldrich).

3-11. Bone marrow transplantation

BM transplantation was performed as previously described²⁷. Donor BM cells from EP3 KO mice and their WT counterparts were harvested and the BM mononuclear cells from each donor (2.0×10^6 cells in 200 mL PBS) were injected into

the tail veins of WT mice irradiated with 9.0 Gy using an MBR-1505R X-ray irradiator (Hitachi Medico Co., Tokyo, Japan) with a filter (copper, 0.5 mm; aluminum, 2 mm), while monitoring the cumulative radiation dose.

3-12. BM-derived dendritic cells and cell culture

Bone marrow cells were isolated from the femur and tibia of WT or EP3 KO mice. The cells were cultured (1×10^6 cells/ml; 5 ml/well) in GM-CSF-containing DMEM medium supplemented with 10% FBS at 37.1°C in 5% humidified CO₂ as described²⁸. The culture medium was changed every day to remove non-adherent granulocytes. On Day 8, cells were harvested by light pipetting. More than 90% of the cells expressed CD11c by FACS analysis. DCs were stimulated with PGE₂ (0.1 nM per well) for 3, 6 and 24 hours.

3-13. In vitro SDF-1 and TGFβ1 expression

To assess DCs expression of SDF-1 and TGFβ1 in vitro, DCs were stimulated with PGE₂ and EP1–EP4 agonists for 3, 6 and 24 hours in serum free medium. The culture medium was collected and stored at -20°C until analysis. The medium was used to assess SDF-1 and TGFβ1 levels using specific enzyme-linked immunosorbent assay (ELISA) kits (R&D Systems, Minneapolis, MN). ELISA kits were also used to measure SDF-1 and TGFβ1 levels in the cell culture supernatants. This experiment was performed in duplicate of serum free medium.

3-14. Statistical Analysis

Data are expressed as the means ± s.e.m (SE). Comparisons between multiple groups were performed by analysis of variance (ANOVA) followed by Scheffe's test. Comparisons between two groups were made using Student's t-test. The correlation between the number of DCs and metastasis was analyzed using the χ^2 test. $P < 0.05$ was considered statistically significant.

4. Results

4-1. Survival rate of mice injected with LLC cells plus BD Matrigel

LLC cells (5.0×10^4) were orthotopically injected into the left lung through the intercostal space without open thoracotomy. The time taken for the skin incision and intrapulmonary injection of LLC cells was approximately 30 s per mouse. The immediate operative mortality in mice injected with BD Matrigel[®] was 10% compared with 80% in the absence of BD Matrigel[®] ($P < 0.01$) (Figure.1A). The use of BD Matrigel[®] prevented death due to pneumothorax. The mean survival time of mice injected with LLC-GFP cell was 15 ± 3 days (range, 12–22 days) (Figure.1B), which was significantly longer than that of sham operation mice ($P < 0.0001$). Some mice died 14 days post-injection due to hemothorax caused by enlargement of the primary tumor. By Day 21, most of the mice had died. Further analysis revealed tumor metastasis to the regional lymph nodes in the majority of mice. Primary tumors developed at the site of direct implantation in 95% (45/50) of animals. Typical chronological macroscopic images of the LLC tumors are shown in Figure 1C.

4-2. Time course of regional lymph node metastasis after the injection of LLC-GFP cells plus BD Matrigel

Figure 2A shows a typical loupe image of the primary tumor and a mediastinal lymph node at Day 10 post-LLC-GFP injection. The injected LLC-GFP cells formed colonies in the middle of the left lung, and LLC-GFP cells metastasized to the regional lymph nodes. Further distant lymph node metastases and other organs' metastases were noted at later time points. We next examined regional lymph node metastasis by fluorescence microscopy (Figure 2B). The metastasis rate in mice with a GFP fluorescence-positive regional lymph node was 0% at Day 7 post-LLC-GFP injection. However, the metastasis rates of the GFP fluorescence-positive regional lymph node were increased, 33%, 73%, and 93% at Days 10, 12, and 14, respectively.

Figure 2C shows H&E stained regional lymph nodes. No LLC colonies were observed in the subcapsular sinus of the lymph nodes at Days 3, 5, 7, and 10 post-LLC-GFP cell injection; however, LLC cells were detected in the subcapsular regions at Days 10, 12 and 14 at regional lymph node and no metastatic nodules were observed in distant organs and lymph nodes, including the lung, liver, spleen, adrenal gland, and cervical and subclavian lymph nodes.

4-3. Aspirin treatment reduces regional lymph node metastasis

We next examined the effect of an authentic NSAID, aspirin, on regional lymph node metastasis. Aspirin had no significant effect on the size of the primary tumor at Days 0 and 7 post-LLC-GFP injection (Figure 3A & B). Regional lymph node metastasis was observed in vehicle-treated mice at Days 10, 12, and 14 post-LLC-GFP injection; however, this was inhibited in aspirin-treated mice. The percentage of lymph node metastasis-positive mice in the aspirin-treated group was significantly lower than that in the vehicle-treated group (Figure 3C; $P < 0.0001$). Furthermore, aspirin treatment led to a significant increase in overall survival

(Figure.3D; $P < 0.0001$).

Figure 4A shows typical fluorescence images of lung tissues (with the trachea) from mice bearing GFP-positive LLC cells. We did not detect LLC-GFP cells to fluorescence-positive regional lymph node from vehicle-treated mice at Day 7, but metastases were evident from Day 10 (Figure 4A; upper panels). These results confirm those obtained after H&E staining (described above). We did not detect any GFP-positive metastases in the aspirin-treated group at any time point (Figure 4A; lower panels). These results were confirmed by RT-PCR for GFP, which is a much more sensitive technique (Figure 4B).

4-4. Early expression of COX-2 in premetastatic regional lymph nodes and COX-2-derived PGE₂-EP3 signaling enhances lymph node metastasis

To test the involvement of COX-2-derived PGE₂, there were no significant changes in tumor size in the celecoxib (a COX-2 inhibitor)-treated or vehicle-treated mice at 7 days following the injection of LLC cells (Fig. S1). However, COX-2-expressing cells were identified in the subcapsular region of the regional mediastinal lymph nodes at 1 or 3 days after the LLC cell implantation (Fig. 5A & C). This was confirmed by analysis of mRNA levels in the lymph node tissues (Fig. 5B). There was no obvious metastasis at 7 days after injection of LLC cells (Fig. 5D & E). Regional lymph node metastasis, which was established in vehicle-treated mice at 10, 12, and 14 days after the injection, was prevented by COX-2 inhibitor treatment (Fig. 5D, E & F). Moreover, the percentage of lymph node metastasis-positive mice was significantly reduced by celecoxib treatment (Fig. 5F). COX-2 expression was also suppressed following celecoxib treatment (Fig. 5 A, B, & C). We previously reported that EP3 signaling increased tumor cell growth and metastasis formation^{14, 29}. Therefore, we examined lymph node metastasis formation in EP3 KO mice. The formation of lymph node metastasis in EP3 KO mice 14 days after LLC cell injection was significantly suppressed compared with that in WT mice (Fig. 5G). These results suggested that COX-2-derived PGE₂-EP3 signaling enhanced lymph node metastasis after parenchymal injection of LLC cells.

4-5. COX-2-dependent premetastatic niche formation in regional lymph nodes

Stromal-cell derived factor 1 (SDF-1, CXCL12) and its receptor, CXCR4, play an important role in metastasis³⁰⁻³². Numerous studies show that CXCR4 is the major chemokine receptor expressed in many types of cancer cells, and that the SDF-1/CXCR4 axis plays a major role in the survival, proliferation, migration and adhesion of tumor cells, including colon cancer, breast cancer, non-small cell lung cancer, prostate cancer, melanoma, cholangiocarcinoma, and oral squamous cell carcinoma cells³³⁻⁴⁰.

Moreover, CXCR4-expressing cancer cells preferentially home to organs with high CXCL12 expression, such as the lung, liver and bone marrow, via the blood and lymphatic system^{41, 42}.

In the present study, we examined the expression of CXCR4 in GFP-labeled LLC cells by immunofluorescence, and found that the large population of

GFP-positive LLC cells were also positive for CXCR4 (Fig. 6A). Next, we examined the expression of SDF-1, a ligand for CXCR4, in the regional lymph nodes following LLC cell injection. The expression of GFP in vehicle-treated mice was significantly increased on Days 3 and 5 after LLC cell implantation compared with that in celecoxib-treated mice (Fig. 6B). Prior to the arrival of the injected LLC cells, we observed increased accumulation of SDF-1 expressing cells in the subcapsular regions from 3 and 5 days after LLC cells injection (Fig. 6C). Many of these SDF-1-positive cells were also COX-2-positive (Fig. 6C). At Day 14, LLC cells preferentially accumulated in a COX-2-dependent manner in subcapsular regions rich in SDF-1/COX-2 double positive cells (Fig. 6D). This finding suggested that COX-2-dependent SDF-1 induction increased metastasis to a predetermined location, specifically the subcapsular regions within the lymph node, and was crucial for the establishment of the lymph node premetastatic niche.

4-6. The SDF-1/CXCR4 axis governs the accumulation of LLC cells in the lymph node premetastatic niche

To determine whether SDF-1/CXCR4 axis induces premetastatic niche formation, we injected a CXCR4 antagonist (AMD3100) following the injection of LLC cells. There was no significant difference in tumor size between vehicle- and AMD 3100-treated mice during the experimental period (Fig. 6E). However, lymph node metastasis was completely suppressed in AMD3100- or CXCR4 neutralizing antibody-treated mice on Day 10 and Day 14 after LLC cell injection (Fig. 6F). Furthermore, the accumulation of SDF-1/COX-2 double positive cells in the regional lymph nodes (Fig. S2) was suppressed in AMD3100-treated mice (Fig. 6G). This reduction was also seen in EP3 knockout mice (Fig. 6H and Fig. S2). These results suggested that lymph node metastasis driven by COX-2/EP3 is highly dependent on the SDF-1/CXCR4 axis.

4-7. COX-2-positive DCs accumulate in the lymph node premetastatic niche and produce SDF-1 via EP3 signaling

To clarify the cellular components relevant to premetastatic niche formation, we examined the cell surface marker profiles of COX-2-expressing cells. We found that DC marker-positive cells accumulated in the subcapsular regions of the lymph nodes (Fig. 7A). Among the DC markers, CD11c, which is a type I transmembrane protein, is highly expressed on most dendritic cells. Furthermore, indoleamine 2, 3-dioxygenase (IDO) is also considered to be a good marker for DCs, and PGE₂ was reported to induce IDO in tolerogenic DCs⁴³. In the present study, immunohistochemical analysis revealed that COX-2-positive cells were also positive for CD11c and IDO (Fig. 7A and B). The accumulation of CD11c- and IDO-positive cells was suppressed in celecoxib or AMD3100-treated mice and in EP3 KO mice (Fig. 7C, D). Quantification of CD11c/IDO-positive cells revealed that the reduction in the accumulation of CD11c /IDO-positive cells by COX-2 inhibition, CXCR4 blockade, and lack of EP3 signaling, began at Day 5 or Day 7 after LLC cells injection (Fig. 7E & F). The CD11c-positive cells were also positive for SDF-1 (Fig. 7G), suggesting that DCs

are sources of SDF-1 in the premetastatic niche. To examine whether PGE₂ induces SDF-1 in DCs, we isolated immature myeloid DCs from the bone marrow and cultured them in the presence of PGs. The mRNA and protein levels of SDF-1 increased significantly following PGE₂ stimulation (Fig. S3A and B). To identify the receptor mediating this action, we added EP agonists (EP1–4), which are highly selective for each receptor subtype. SDF-1 protein levels in the culture media increased upon incubation of DCs from WT mice with an EP3 agonist, ONO-AE-248 (Fig. 7H); however, DCs from EP3 KO did not secrete SDF-1 (Fig. 7I). Treatment with EP agonists for EP1, EP2, and EP4 did not increase SDF-1 secretion (Fig. S3C). These results suggested that DCs accumulation in the premetastatic niche is dependent on COX-2-EP3 and SDF-1, and that induction of SDF-1 in DCs is dependent on EP3 signaling.

4-8. EP3 signaling facilitates DCs recruitment to the regional lymph node premetastatic niche

To clarify the process of DCs recruitment to the premetastatic niche, we injected mice intravenously with GFP⁺DC cells following the injection of GFP⁺LLC cells. The GFP⁺DCs from WT mice were recruited to the subcapsular regions at Day 10 (Fig. 8A). This accumulation was significantly reduced following injection of GFP⁺DC cells from EP3 KO mice (Fig. 8A). The WT DCs recruited to the subcapsular regions expressed higher levels of SDF-1 than those from EP3 KO mice. The percentage of lymph node metastasis was higher following the injection of WT DCs than after the injection of vehicle or EP3 KO DCs (Fig. 8B). Most of the accumulated DCs were CXCR4-positive (Fig. 8C), suggesting that the DCs expressing EP3 enhanced the recruitment of DCs via the generation of SDF-1. These findings imply a positive feedback loop in the EP3/SDF-1 interplay.

4-9. Both COX-2/EP3 signaling and SDF-1 increase the recruitment of Tregs to the lymph node premetastatic niche

Previous studies show that the increased production of PGE₂ by tumors is associated with the induction of Tregs and with T cell inhibition^{44, 45}. Moreover, increased Tregs numbers have been reported for various cancers, including lung, liver, pancreas, ovary, and head and neck. In the present study, we examined whether COX-2 inhibition could reduce Tregs recruitment to the regional lymph nodes. As shown in Fig. 9A, a substantial number of Foxp3⁺Tregs accumulated in the subcapsular regions of the regional lymph nodes, which was suppressed by COX-2 inhibition, CXCR4 blockade, and a lack of EP3 signaling. These results were confirmed by quantitative analysis (Fig. 9B), and immunofluorescent analysis (Fig. S4A & B). Taken together, these findings suggest that the accumulation of Tregs in lymph nodes is dependent on both COX-2/EP3 signaling and the SDF-1/CXCR4 axis. Since many of the Foxp3-positive cells expressed CXCR4 (Fig. S4C), it is possible that DC-derived SDF-1 may attract Tregs to the premetastatic niche. It was previously reported that immature DCs secrete TGFβ to induce Treg proliferation⁴⁶. Therefore, to examine whether TGFβ1 was secreted by DCs in the premetastatic niche, we

performed immunofluorescence analysis of TGF β 1 expression by CD11c⁺DCs. We found that CD11c-positive cells expressed TGF β 1 and that the number of CD11c/TGF β 1 double positive cells was reduced in EP3 KO mice compared with that in WT mice (Fig. 9C). We also measured TGF β 1 secretion by DCs cultured in the presence of an EP3 agonist. WT DCs secreted large amounts of TGF β 1 in response to EP3 stimulation, but DCs from EP3 KO mice did not (Fig.9D). TGF β expression was significantly suppressed in COX-2 inhibitor- or AMD3100-treated mice and in EP3 KO mice (Fig. 9E). These results suggested that the accumulation of Tregs in the premetastatic niche was COX-2/EP3- and SDF-1/ CXCR4-dependent, and that the accumulated Tregs might influence the fate of the tumor cells colonizing the premetastatic niche.

4-10. PGE₂-EP3 signaling as a regulator of lymph node lymphangiogenesis

Once the metastatic cells arrive at the lymph nodes, lymph node lymphangiogenesis may facilitate further metastasis to other organs, such as the distal lymph nodes and lungs. It was reported that no metastases were observed in distant organs in the absence of lymph node metastases⁴⁷. We determined the expression of prolymphangiogenic growth factors, VEGF-C and VEGF-D, in the regional lymph nodes and found that the gene expression of these growth factors was significantly increased prior to the arrival of the LLC cells, but was suppressed in Celecoxib-treated mice and in EP3 KO mice (Fig. 10A and B). Moreover, VEGFR-3, expressed on lymphatic endothelial cells, was increased in the regional lymph nodes from Day 3, but was reduced in COX-2-treated mice and EP3 KO mice (Fig. 10C). This suggests that COX-2/EP3-dependent induction of VEGF-C/D plays a role in lymphangiogenesis in the regional lymph nodes. Indeed, LYVE-1 immunostaining revealed that lymphatic structures increased from Day 3, mainly in the efferent region of the lymph nodes, and that this increase was suppressed by celecoxib treatment (Fig. 10D). These results suggested that PGE₂-EP3 signaling induces lymphangiogenesis in regional metastatic lymph nodes before the arrival of LLC cells.

We considered that a schematic presentation of COX-2/SDF-1- dependent premetastatic niche formation. COX-2 and EP3 mediate the increase of SDF-1 at the premetastatic site prior to the arrival of tumor cells to the regional lymph node. CXCR4-positive tumor cells become mobilized to SDF-1 generating sites. Simultaneously, CXCR4/EP3-positive dendritic cells are recruited to generate SDF-1 in response to EP3 signaling. (Fig. 10E) When the metastasized LLC cells were fate, Tregs are recruited to the premetastatic niche via SDF-1/EP3-signaling. The dendritic cells recruited to the premetastatic niche secrete TGF β 1 in an EP3/SDF-1-dependent manner. Thus, COX-2-PGE₂ -EP3 signaling together with SDF-1/CXCR4 signaling may decide the fate of the colonizing LLC cells. Moreover, COX-2/EP3 signaling up-regulates lymph node lymphangiogenesis. Together, these events may facilitate tumor cell growth in the regional lymph nodes and lymph node or systemic metastasis. (Fig. 10F)

5. Discussion

Our study demonstrated that the formation of the premetastatic niche in regional lymph nodes is dependent on COX-2/PGE₂-EP3 signaling, and that SDF-1-expressing DCs have a significant effect on the accumulation of CXCR4-expressing LLC cells. COX-2/EP3-dependent induction was initiated from the early stage in which there is no metastasis in regional lymph node. EP3 signaling was also active to accumulate DCs in subcapsular regions of lymph node for future accumulation of LLC cells. We observed an increase in the release of SDF-1 from DCs in lymph nodes following LLC cell injection. In addition, we observed significant Tregs recruitment to the premetastatic niche; this process was dependent on COX-2/EP3 and SDF-1. Lymph node lymphangiogenesis, which may facilitate further metastasis, was also induced in a COX-2/EP3-dependent manner. These findings indicate that prostanoid signaling plays a significant role in lymph node metastasis.

Prostanoids, including prostaglandins, are generated from arachidonic acid, a process regulated by the rate-limiting COX enzymes. COX-2 can be induced in most tissues, where it mediates the production of pro-inflammatory PGs during inflammation and in tumorigenic settings. Neoplastic tissues, such as human colon cancers, contain high concentrations of PGs, and the pro-tumorigenic effects of COX-2 are largely attributed to its role in PGE₂ production²⁴. COX-2 expression is associated with poor patient prognosis and survival^{48, 49}. We previously reported that, in addition to tumor COX-2 expression, COX-2 present in stromal tissues had a significant effect on tumor-associated angiogenesis⁵⁰. Further studies showed that COX-2 induced lung metastasis via EP3 signaling²⁹. However, little is known about the involvement of COX-2 and PG receptors in lymph node metastasis. The present study reveals for the first time that COX-2 and EP3 signaling play a role in lymph node metastasis, and shows that COX-2 and EP3 signaling mediate the induction of SDF-1 and CXCR4 to establish the premetastatic niche.

The cellular components involved in the formation of premetastatic niches are largely unknown. In the present study, we showed that DCs play an important role in the formation of the lymph node premetastatic niche. DCs are bone marrow-derived cells that are present in all tissues^{51, 52}. Mouse models of cancer reveal that DCs capture tumor antigens released from tumor cells and cross-present these antigens to T cells in the tumor-draining lymph nodes, thereby generating tumor-specific cytotoxic T lymphocytes, which play a role in tumor rejection^{53, 54}. DCs sample the environment and transmit the gathered information to cells of the adaptive immune system (T cells and B cells). DC differentiation from hematopoietic stem cells (HSCs) and DC function are sensitive to lipid mediators, such as prostaglandins, and DCs express several receptors involved in prostaglandin signaling pathways⁵⁵. PGE₂ is a key modulator of DC differentiation, maturation, migration, and cytokine production⁵⁶⁻⁶⁰. In contrast to its inhibitory effects on monocytes, PGE₂ activates immature DCs. As a first step towards the transition from an adhesive to a highly migratory state, DCs lose their specific integrin- and actin-rich adhesive structures, called podosomes, within minutes following PGE₂ stimulation⁵⁹. This rapid response to PGE₂ is mediated by increased

cAMP intracellular levels, activation of the small GTPase RhoA, and subsequent induction of actomyosin contraction, ultimately leading to rapid podosome dissolution⁶⁰. In the present study, we identified a novel function of DCs in premetastatic niche formation in the regional lymph nodes in tumor bearing mice. As shown in Fig. 7A and B, COX-2 induction in DCs was observed at the early stages of the experiment, suggesting that COX-2 might regulate the formation of the premetastatic niche in the regional lymph nodes. SDF-1 induction in DCs was dependent on COX-2 and EP3 signaling, and blockade of the SDF-1/CXCR4 axis suppressed the formation of the premetastatic niche. In vitro assays using isolated DCs showed that EP3 signaling up-regulated SDF-1 expression (Fig. 7H and I). These findings revealed the crucial role of COX-2 and EP3 signaling in the formation of premetastatic niche via the SDF-1/CXCR4 chemokine axis.

We further demonstrated that Tregs were recruited to the regional lymph nodes via COX-2/EP3 and SDF-1. Tregs, formerly known as suppressor T cells, are a subpopulation of T cells that modulate the immune system, maintain tolerance to self-antigens, and abrogate the development of autoimmune disease⁶¹. Studies in mouse models revealed the potential of Tregs for the treatment of autoimmune diseases and cancer, and for organ transplantation. As shown in Fig. 9B, the recruitment of Tregs was observed in the regional lymph node premetastatic niche, and it was suppressed by COX-2 inhibition, EP3 blockade, and SDF-1 blockade. This is a novel finding, showing the interplay between prostanoids and Tregs. Tregs expressed CXCR4 (Fig. S4D); thus, SDF-1 secreted by DCs may act as a major attractant of Tregs to the premetastatic niche. This may increase the immunosuppressive potential of Tregs and facilitate further metastasis.

We previously reported that lymphangiogenesis in a Matrigel subcutaneous implantation model, which mimics tumor stromal reactions, was enhanced by COX-2 and EP3/4 signaling¹⁵. In addition, topical implantation of both VEGF-C- and VEGF-A-overexpressing tumor cells induced lymphangiogenesis in sentinel lymph nodes⁴⁷. However, a more precise evaluation of lymph node lymphangiogenesis showed that lymphangiogenesis took place in the efferent lymphatic area, whereas the premetastatic niche was formed in the subcapsular regions of the sentinel lymph nodes. We previously reported that PGE₂ stimulated the induction of VEGF-A/C, and that VEGF-A induced COX-2^{15, 16, 62, 63}. COX-2/EP3-dependent induction of SDF-1 in DCs localized in subcapsular regions may induce formation of the premetastatic niche for future colonization by LLC cells. It will be important to determine the exact mechanisms by which lymph node lymphangiogenesis induces further tumor cell metastasis to the lymph nodes and other tissues. Although the induction of lymph node lymphangiogenesis and subsequent dendritic cell motility following adjuvant-induced skin inflammation has been described⁶⁴, our study demonstrated that COX-2-positive SDF-1-producing DCs are the major cell component driving niche formation, whereas PGs regulate lymph node lymphangiogenesis. Lymph node lymphangiogenesis may decide the fate of the colonizing tumor cells, and blockade of PG biosynthesis and receptor signaling may prevent further tumor cell metastasis to the lymph nodes and other tissues.

6. Conclusion

In conclusion, our study shows that endogenous COX-2-derived PGE₂ stimulated the EP3 receptor on DCs, leading to the up-regulation of SDF-1 expression in the subcapsular regions in regional lymph nodes following LLC cell injection into the lungs. SDF-1 up-regulation facilitated the accumulation of CXCR4⁺ LLC cells and the formation of the regional lymph node premetastatic niche. We also found that accumulation of regulatory T cells and lymph node lymphangiogenesis, both of which may decide the fate of metastasized tumor cells, were COX-2/EP3-dependent. Taken together, our findings suggest that PGE₂ inhibitors, together with SDF-1 receptor antagonists and EP3 antagonists, may be promising agents for the suppression of premetastatic niche formation and lymph node metastasis.

7. Prospective

In this study, we investigated lymph node metastasis on lung cancer related with COX-2 derived PGE₂ stimulated the EP3 receptor on DCs, leading to the up-regulation of SDF-1 expression, premetastatic niche formation in the subcapsular regions using with mice model. However, because this study was experimental injected tumor model, when we say closely it is not spontaneous tumor lymph node metastasis model, we will apply these results to clinical research and investigate the evaluation in clinical research in future, associated with COX-2 derived PGE₂-EP3 signaling, SDF-1/CXCR4 axis and immunotherapy. We think that we can contribute to improvement of the lung cancer prognosis if even a person can actually prove this.

8. References

1. Jemal A, Siegel R, Xu J and Ward E. Cancer statistics, 2010. *CA: a cancer journal for clinicians*. 2010; 60: 277-300.
2. Siegel R, Naishadham D and Jemal A. Cancer statistics, 2012. *CA: a cancer journal for clinicians*. 2012; 62: 10-29.
3. Howlader N NA, Krapcho M, Garshell J, Neyman N, Altekruse SF, Kosary CL, Yu M, Ruhl J, Tatalovich Z, Cho H, Mariotto A, Lewis DR, Chen HS, Feuer EJ, Cronin KA (eds). *SEER Cancer Statistics Review 1975-2010*. Cancer Statistics. 2013.
4. Sandler A, Gray R, Perry MC, et al. Paclitaxel-carboplatin alone or with bevacizumab for non-small-cell lung cancer. *The New England journal of medicine*. 2006; 355: 2542-50.
5. Chaffer CL and Weinberg RA. A perspective on cancer cell metastasis. *Science*. 2011; 331: 1559-64.
6. Fidler IJ. The pathogenesis of cancer metastasis: the 'seed and soil' hypothesis revisited. *Nature reviews Cancer*. 2003; 3: 453-8.
7. Joyce JA and Pollard JW. Microenvironmental regulation of metastasis. *Nature reviews Cancer*. 2009; 9: 239-52.
8. Pepper MS. Lymphangiogenesis and tumor metastasis: myth or reality? *Clin Cancer Res*. 2001; 7: 462-8.
9. Paget S. The distribution of secondary growths in cancer of the breast. 1889. *Cancer metastasis reviews*. 1989; 8: 98-101.
10. Hiratsuka S, Watanabe A, Sakurai Y, et al. The S100A8-serum amyloid A3-TLR4 paracrine cascade establishes a pre-metastatic phase. *Nature cell biology*. 2008; 10: 1349-55.
11. Kaplan RN, Riba RD, Zacharoulis S, et al. VEGFR1-positive haematopoietic bone marrow progenitors initiate the pre-metastatic niche. *Nature*. 2005; 438: 820-7.
12. Kim M, Koh YJ, Kim KE, et al. CXCR4 signaling regulates metastasis of chemoresistant melanoma cells by a lymphatic metastatic niche. *Cancer research*. 2010; 70: 10411-21.
13. Dannenberg AJ and Subbaramaiah K. Targeting cyclooxygenase-2 in human neoplasia: rationale and promise. *Cancer cell*. 2003; 4: 431-6.
14. Amano H, Hayashi I, Endo H, et al. Host prostaglandin E(2)-EP3 signaling regulates tumor-associated angiogenesis and tumor growth. *The Journal of experimental medicine*. 2003; 197: 221-32.
15. Hosono K, Suzuki T, Tamaki H, et al. Roles of prostaglandin E2-EP3/EP4 receptor signaling in the enhancement of lymphangiogenesis during fibroblast growth factor-2-induced granulation formation. *Arteriosclerosis, thrombosis, and vascular biology*. 2011; 31: 1049-58.
16. Kashiwagi S HK, Suzuki T, Takeda A, Uchinuma E, Majima M. Role of COX-2 in lymphangiogenesis and restoration of lymphatic flow in secondary lymphedema.

- Laboratory investigation; a journal of technical methods and pathology. 2011; 91: 12.
17. Katoh H, Hosono K, Ito Y, et al. COX-2 and prostaglandin EP3/EP4 signaling regulate the tumor stromal proangiogenic microenvironment via CXCL12-CXCR4 chemokine systems. *The American journal of pathology*. 2010; 176: 1469-83.
 18. Kubo H, Hosono K, Suzuki T, et al. Host prostaglandin EP3 receptor signaling relevant to tumor-associated lymphangiogenesis. *Biomed Pharmacother*. 2010; 64: 101-6.
 19. Majima M, Amano H and Hayashi I. Prostanoid receptor signaling relevant to tumor growth and angiogenesis. *Trends in pharmacological sciences*. 2003; 24: 524-9.
 20. Oshima M, Dinchuk JE, Kargman SL, et al. Suppression of intestinal polyposis in Apc delta716 knockout mice by inhibition of cyclooxygenase 2 (COX-2). *Cell*. 1996; 87: 803-9.
 21. Thun MJ HS, Patrono C. Nonsteroidal anti-inflammatory drugs as anticancer agents: mechanistic, pharmacologic, and clinical issues. *J Natl Cancer Inst*. 2002; 94: 252-66.
 22. Wilson NS and Villadangos JA. Regulation of antigen presentation and cross-presentation in the dendritic cell network: facts, hypothesis, and immunological implications. *Advances in immunology*. 2005; 86: 241-305.
 23. Braun D, Longman RS and Albert ML. A two-step induction of indoleamine 2,3 dioxygenase (IDO) activity during dendritic-cell maturation. *Blood*. 2005; 106: 2375-81.
 24. Greenhough A, Smartt HJ, Moore AE, et al. The COX-2/PGE2 pathway: key roles in the hallmarks of cancer and adaptation to the tumour microenvironment. *Carcinogenesis*. 2009; 30: 377-86.
 25. Sombroek CC, Stam AG, Masterson AJ, et al. Prostanoids play a major role in the primary tumor-induced inhibition of dendritic cell differentiation. *J Immunol*. 2002; 168: 4333-43.
 26. Trinath J, Hegde P, Sharma M, et al. Intravenous immunoglobulin expands regulatory T cells via induction of cyclooxygenase-2-dependent prostaglandin E2 in human dendritic cells. *Blood*. 2013; 122: 1419-27.
 27. Ogawa Y, Suzuki T, Oikawa A, et al. Bone marrow-derived EP3-expressing stromal cells enhance tumor-associated angiogenesis and tumor growth. *Biochemical and biophysical research communications*. 2009; 382: 720-5.
 28. Lutz MB, Kukutsch NA, Menges M, Rossner S and Schuler G. Culture of bone marrow cells in GM-CSF plus high doses of lipopolysaccharide generates exclusively immature dendritic cells which induce alloantigen-specific CD4 T cell anergy in vitro. *European journal of immunology*. 2000; 30: 1048-52.
 29. Amano H, Ito Y, Suzuki T, et al. Roles of a prostaglandin E-type receptor, EP3, in upregulation of matrix metalloproteinase-9 and vascular endothelial growth factor during enhancement of tumor metastasis. *Cancer Sci*. 2009; 100: 2318-24.
 30. Arya M, Ahmed H, Silhi N, Williamson M and Patel HR. Clinical importance and therapeutic implications of the pivotal CXCL12-CXCR4 (chemokine

- ligand-receptor) interaction in cancer cell migration. *Tumour biology : the journal of the International Society for Oncodevelopmental Biology and Medicine*. 2007; 28: 123-31.
31. Sun X, Cheng G, Hao M, et al. CXCL12 / CXCR4 / CXCR7 chemokine axis and cancer progression. *Cancer metastasis reviews*. 2010; 29: 709-22.
 32. Teicher BA and Fricker SP. CXCL12 (SDF-1)/CXCR4 pathway in cancer. *Clin Cancer Res*. 2010; 16: 2927-31.
 33. Zeelenberg IS, Ruuls-Van Stalle L and Roos E. The chemokine receptor CXCR4 is required for outgrowth of colon carcinoma micrometastases. *Cancer research*. 2003; 63: 3833-9.
 34. Bachelder RE, Wendt MA and Mercurio AM. Vascular endothelial growth factor promotes breast carcinoma invasion in an autocrine manner by regulating the chemokine receptor CXCR4. *Cancer research*. 2002; 62: 7203-6.
 35. Belperio JA, Phillips RJ, Burdick MD, Lutz M, Keane M and Strieter R. The SDF-1/CXCL 12/CXCR4 biological axis in non-small cell lung cancer metastases. *Chest*. 2004; 125: 156S.
 36. Burger M, Glodek A, Hartmann T, et al. Functional expression of CXCR4 (CD184) on small-cell lung cancer cells mediates migration, integrin activation, and adhesion to stromal cells. *Oncogene*. 2003; 22: 8093-101.
 37. Singh S, Singh UP, Grizzle WE and Lillard JW, Jr. CXCL12-CXCR4 interactions modulate prostate cancer cell migration, metalloproteinase expression and invasion. *Laboratory investigation; a journal of technical methods and pathology*. 2004; 84: 1666-76.
 38. Scala S, Ottaiano A, Ascierto PA, et al. Expression of CXCR4 predicts poor prognosis in patients with malignant melanoma. *Clin Cancer Res*. 2005; 11: 1835-41.
 39. Gentilini A, Rombouts K, Galastri S, et al. Role of the stromal-derived factor-1 (SDF-1)-CXCR4 axis in the interaction between hepatic stellate cells and cholangiocarcinoma. *J Hepatol*. 2012; 57: 813-20.
 40. Uchida D, Begum NM, Almofti A, et al. Possible role of stromal-cell-derived factor-1/CXCR4 signaling on lymph node metastasis of oral squamous cell carcinoma. *Experimental cell research*. 2003; 290: 289-302.
 41. Albrecht I and Christofori G. Molecular mechanisms of lymphangiogenesis in development and cancer. *The International journal of developmental biology*. 2011; 55: 483-94.
 42. Burger JA and Kipps TJ. CXCR4: a key receptor in the crosstalk between tumor cells and their microenvironment. *Blood*. 2006; 107: 1761-7.
 43. von Bergwelt-Baildon MS, Popov A, Saric T, et al. CD25 and indoleamine 2,3-dioxygenase are up-regulated by prostaglandin E2 and expressed by tumor-associated dendritic cells in vivo: additional mechanisms of T-cell inhibition. *Blood*. 2006; 108: 228-37.
 44. Baratelli F, Lin Y, Zhu L, et al. Prostaglandin E2 induces FOXP3 gene expression and T regulatory cell function in human CD4+ T cells. *J Immunol*. 2005; 175: 1483-90.

45. Sharma S, Yang SC, Zhu L, et al. Tumor cyclooxygenase-2/prostaglandin E2-dependent promotion of FOXP3 expression and CD4+ CD25+ T regulatory cell activities in lung cancer. *Cancer research*. 2005; 65: 5211-20.
46. Ghiringhelli F, Puig PE, Roux S, et al. Tumor cells convert immature myeloid dendritic cells into TGF-beta-secreting cells inducing CD4+CD25+ regulatory T cell proliferation. *The Journal of experimental medicine*. 2005; 202: 919-29.
47. Hirakawa S, Brown LF, Kodama S, Paavonen K, Alitalo K and Detmar M. VEGF-C-induced lymphangiogenesis in sentinel lymph nodes promotes tumor metastasis to distant sites. *Blood*. 2007; 109: 1010-7.
48. Khuri FR, Wu H, Lee JJ, et al. Cyclooxygenase-2 overexpression is a marker of poor prognosis in stage I non-small cell lung cancer. *Clin Cancer Res*. 2001; 7: 861-7.
49. Peng L, Zhou Y, Wang Y, Mou H and Zhao Q. Prognostic significance of COX-2 immunohistochemical expression in colorectal cancer: a meta-analysis of the literature. *Plos One*. 2013; 8: e58891.
50. Yoshida S, Amano H, Hayashi I, et al. COX-2/VEGF-dependent facilitation of tumor-associated angiogenesis and tumor growth in vivo. *Laboratory investigation; a journal of technical methods and pathology*. 2003; 83: 1385-94.
51. Banchereau J and Steinman RM. Dendritic cells and the control of immunity. *Nature*. 1998; 392: 245-52.
52. Steinman RM and Banchereau J. Taking dendritic cells into medicine. *Nature*. 2007; 449: 419-26.
53. Diamond MS, Kinder M, Matsushita H, et al. Type I interferon is selectively required by dendritic cells for immune rejection of tumors. *The Journal of experimental medicine*. 2011; 208: 1989-2003.
54. Fuertes MB, Kacha AK, Kline J, et al. Host type I IFN signals are required for antitumor CD8+ T cell responses through CD8{alpha}+ dendritic cells. *The Journal of experimental medicine*. 2011; 208: 2005-16.
55. Gualde N and Harizi H. Prostanoids and their receptors that modulate dendritic cell-mediated immunity. *Immunology and cell biology*. 2004; 82: 353-60.
56. Khayrullina T, Yen JH, Jing H and Ganea D. In vitro differentiation of dendritic cells in the presence of prostaglandin E2 alters the IL-12/IL-23 balance and promotes differentiation of Th17 cells. *J Immunol*. 2008; 181: 721-35.
57. Legler DF, Krause P, Scandella E, Singer E and Groettrup M. Prostaglandin E2 is generally required for human dendritic cell migration and exerts its effect via EP2 and EP4 receptors. *J Immunol*. 2006; 176: 966-73.
58. Singh P, Hoggatt J, Hu P, et al. Blockade of prostaglandin E2 signaling through EP1 and EP3 receptors attenuates Flt3L-dependent dendritic cell development from hematopoietic progenitor cells. *Blood*. 2012; 119: 1671-82.
59. van Helden SF, Krooshoop DJ, Broers KC, Raymakers RA, Figdor CG and van Leeuwen FN. A critical role for prostaglandin E2 in podosome dissolution and induction of high-speed migration during dendritic cell maturation. *J Immunol*. 2006; 177: 1567-74.

60. van Helden SF, Oud MM, Joosten B, Peterse N, Figdor CG and van Leeuwen FN. PGE2-mediated podosome loss in dendritic cells is dependent on actomyosin contraction downstream of the RhoA-Rho-kinase axis. *Journal of cell science*. 2008; 121: 1096-106.
61. Hori S, Nomura T and Sakaguchi S. Control of regulatory T cell development by the transcription factor Foxp3. *Science*. 2003; 299: 1057-61.
62. Amano H, Hayashi I, Ando K, Minamida S, Yoshimura H and Majima M. Adenylate cyclase/protein kinase A signaling pathway enhances angiogenesis through induction of vascular endothelial growth factor in vivo. *Japanese journal of pharmacology*. 2002; 88: 179p-p.
63. Majima M, Hayashi I, Muramatsu M, Katada J, Yamashina S and Katori M. Cyclo-oxygenase-2 enhances basic fibroblast growth factor-induced angiogenesis through induction of vascular endothelial growth factor in rat sponge implants. *Brit J Pharmacol*. 2000; 130: 641-9.
64. Angeli V, Ginhoux F, Llodra J, et al. B cell-driven lymphangiogenesis in inflamed lymph nodes enhances dendritic cell mobilization. *Immunity*. 2006; 24: 203-15.

9. Figure Legends

9-1. Figure 1. Regional lymph node metastasis model.

- (A) Survival of mice injected with LLC-GFP in the presence or absence of Matrigel[®]. The group without Matrigel[®] showed a significantly lower survival rate ($P < 0.01$, $N = 20$ per group). The Chi-squared test was used to evaluate significant differences.
- (B) Overall survival of mice in the sham (PBS + Matrigel[®]) and LLC-treated (LLC-GFP + Matrigel[®]) groups. The survival rate was significantly lower in the LLC-treated group ($P < 0.0001$; Log-rank test).
- (C) Typical macroscopic images of primary tumors formed over time after LLC-GFP cell injection. The primary tumor showed a gradual increase in size.

9-2. Figure 2. Time course of regional lymph node metastasis after the injection of LLC plus Matrigel.

- (A) Typical loupe image at Day 10. Typical H&E staining pattern after LLC-GFP cell injection. Bars; 5 mm. PT: Primary Tumor, LN: Lymph Node, T: Thymus.
- (B) Time course showing the percentage of mice with GFP-positive metastases in the regional lymph nodes. Metastasis was detected 10 days after the LLC-GFP cell injections. On Day 14, most of the LLC-injected mice showed regional/mediastinal lymph node metastasis.
- (C) Typical H&E staining pattern in the regional lymph nodes from mice injected with LLC cells. No LLC cell colonies were detected in the subcapsular regions at Day 10. However, metastases were detected in the subcapsular regions of the lymph nodes at Days 12 and 14 post-LLC cell injection. T: LLC cells.

9-3. Figure 3. Effect of aspirin on regional lymph node metastasis.

- (A) Temporal changes in LLC-GFP tumor size in the lungs. The results from vehicle-treated mice were compared with those from aspirin-treated mice. Aspirin was given orally (100 mg/kg, twice a day) throughout the experimental period. There was no significant difference in tumor size between the groups. Vehicle-treated group; $N = 15$. Aspirin-treated group; $N = 10$. Data are expressed as the mean \pm S.E. ANOVA was used to determine significant differences.
- (B) Typical loupe images after LLC-GFP cell injection, vehicle-only injection (upper panels), and aspirin treatment (lower panels). Bars; 50 mm. Blue arrow; primary tumor, red arrow; mediastinal lymph node, green arrow; thymus.
- (C) Temporal changes in the percentage of mice showing regional lymph node metastasis. Metastasis was compared in the LLC-GFP cell injected, vehicle-treated, and aspirin-treated groups. There was significant difference between the groups. Vehicle group; $N = 15$. Aspirin-treated group; $N = 10$. $P < 0.05$ (χ^2 test).
- (D) Overall survival of mice in the vehicle-treated and aspirin-treated groups. Mice in the aspirin-treated group showed improved survival ($P < 0.0001$; Log-rank test).

9-4. Figure 4. Effect of aspirin on GFP-positive LLC cell growth and the expression of GFP in the regional lymph nodes.

- (A) Typical Images of lungs and regional lymph nodes taken under a fluorescence microscope. LLC-GFP cells were detected in the regional lymph node 10 days after LCC-GFP injection. Aspirin treatment (100 mg/kg, twice a day) markedly suppressed the accumulation of GFP-positive cells. Bars; 5 mm. PT: Primary Tumor, LN: Lymph Node.
- (B) Real-time PCR analysis of GFP expression. GFP mRNA levels were measured in isolated regional lymph nodes by real-time PCR. There was a significant reduction in GFP expression in aspirin-treated mice compared with vehicle-treated mice. Vehicle-treated group, N = 15; Aspirin-treated group, N = 10. Data are expressed as the mean \pm S.E ($P < 0.05$; ANOVA, overall and $P < 0.05$; Student's t-test, each days).

9-5. Figure 5. COX-2 induction in regional lymph nodes and the effect of COX-2 inhibition on regional lymph node metastasis

- (A) Immunohistochemical staining of the regional lymph nodes with a COX-2 antibody after lung LLC cell implantation. In vehicle-treated mice, COX-2 positive cells (indicated by arrows) were localized in the subcapsular regions. Celecoxib, a COX-2 inhibitor, was given orally (100mg/kg/ day) throughout the experimental period. Bars; 50 mm. S; subcapsular regions, C; cortex.
- (B) Real time PCR analysis of COX-2. COX-2 mRNA levels in the isolated regional lymph nodes were determined by real time PCR. COX-2 was detected in the regional lymph nodes of vehicle-treated mice from day 1 after LLC cells injection. COX-2 mRNA levels were significantly reduced in the celecoxib-treated group compared with the vehicle-treated group. N=15 per group. Error bars indicate the mean \pm SE. $P < 0.0001$ (ANOVA).
- (C) COX-2 positive cell population (%) in the subcapsular regions. The percent total cell population was significantly reduced in the celecoxib-treated group after LLC cell implantation compared to with the vehicle-treated group. N=15 per group. Error bars indicate the mean \pm SE. $P < 0.0001$ (ANOVA).
- (D) Loupe images obtained on Day 10. Typical H.E. staining after LLC cell implantation. Bars; 5 mm. PT: Primary Tumor, LN: Lymph Node, T: Thymus.
- (E) Fluorescence microscope images obtained after implantation of GFP-positive LLC cells into the lung. Bars; 3 mm. PT: Primary Tumor, LN: Lymph Node.
- (F) Temporal changes in the percentage of regional lymph node metastasis-positive mice. Metastasis after LLC cell implantation into the vehicle-treated group was compared with that in celecoxib-treated group. N=15 per group. $P < 0.05$ (χ^2 test).
- (G) Percentage of regional lymph node metastasis-positive mice. Metastasis after LLC cell implantation was compared between EP3 KO mice and wild type (WT) mice. Wild; N=15, EP3 KO; N=5. $P < 0.05$ (χ^2 test).

9-6. Figure 6. COX-2/EP3 enhances SDF-1 expression in lymph nodes

- (A) Immunofluorescence images of CXCR4 expression in cultured GFP-positive LLC cells. Bar; 20 μ m.
- (B) Temporal changes in the SDF-1 positive cell population in the regional lymph nodes after LLC implantation in celecoxib-treated mice were compared with those in vehicle-treated mice. A COX-2 inhibitor, celecoxib was given orally (100mg/kg/day) throughout the experimental period. N=15 per group. $P < 0.05$ (χ^2 test).
- (C) Immunofluorescence images showing COX-2/SDF-1 double staining in the regional lymph nodes after LLC cells implantation. COX-2/SDF-1 double positive cells accumulated before the arrival of GFP-negative LLC cells. Celecoxib treatment strongly inhibited the accumulation of double positive cells. Naïve; images from mice with no treatment. Bars; 50 μ m. S; subcapsular regions, C; cortical regions.
- (D) Accumulation of SDF-1/GFP double positive LLC cells in the subcapsular regions in regional lymph nodes at Day 14. Celecoxib treatment reduced the accumulation of SDF-1/GFP double positive cells. Bars; 50 μ m. EX; extracellular matrix, S; subcapsular regions, C; cortical regions.
- (E) Temporal changes in LLC tumor size in the lungs from vehicle-treated mice and AMD3100-treated mice. A CXCR4 antagonist, AMD3100, was given orally (10 mg/kg/day) throughout the experimental period. Vehicle group; N=15. AMD3100 group; N=10. Error bars indicate the mean \pm SE. ANOVA was used to evaluate significance.
- (F) Temporal changes in the percentage of regional lymph node metastasis-positive mice following vehicle or AMD3100 treatment. In some mice, a CXCR4 neutralizing antibody was given throughout the experimental period (100mg/day). Vehicle group; N=15. AMD3100 group; N=10; CXCR4 neutralizing antibody group; N=5. $P < 0.05$ (χ^2 test).
- (G) Temporal changes in the SDF-1 positive cell population in the regional lymph nodes after LLC implantation. The results from AMD3100-treated mice were compared with those from vehicle mice. Vehicle group; N=15. AMD3100 group; N=10. Error bars indicate the mean \pm SE. $P < 0.0001$ (ANOVA). Student's t-test was used to evaluate significant differences at Days 3 and 5 ($P < 0.05$).
- (H) Temporal changes in the SDF-1 positive cell population in the regional lymph nodes after LLC implantation. The results from EP3 KO mice were compared with those from WT mice. Wild type; N=15; EP3 KO; N=5. Error bars indicate the mean \pm SE. $P < 0.0001$ (ANOVA). $P < 0.05$ (Student's t-test).

9-7. Figure 7. Effect of the SDF-1/CXCR4 axis on lymph node metastasis

- (A) COX-2/CD11c double immunofluorescent staining of the subcapsular regions in regional lymph nodes 7 days after LLC implantation. Bar; 20 μ m. S; subcapsular regions, C; cortical regions.
- (B) COX-2/ IDO double immunofluorescent staining of the subcapsular regions in regional lymph node 7 days after LLC implantation. Bar; 20 μ m. S; subcapsular regions, C; cortical regions.
- (C) Localization of CD11c-positive cells in the subcapsular regions in regional lymph node 7 days after LLC implantation. Vehicle, a typical result from vehicle-treated mice; AMD3100, a typical result from AMD3100-treated mice; EP3 KO, a typical result from EP3 KO mice. Bar; 50 μ m. S; subcapsular regions, C; cortical regions.
- (D) Localization of IDO-positive cells in the subcapsular regions in regional lymph node 7 days after LLC implantation. The experimental conditions were the same as those in panel C. Bar; 50 μ m.
- (E) Temporal changes in the CD11c-positive cell population in the regional lymph nodes after LLC implantation. The results from celecoxib-treated mice, AMD3100-treated mice, and EP3 KO mice were compared with those from vehicle-treated mice. Vehicle group; N=15. Celecoxib group; N=15. AMD3100 group; N=10. EP3 KO; N=5. Error bars indicate the mean \pm SE. $P < 0.0001$ (ANOVA). Student's t-test was used to evaluate significant differences at Days 3, 5 and 7 after LLC implantation ($P < 0.05$).
- (F) Temporal changes in the IDO-positive cell population in the regional lymph nodes after LLC implantation. The results from celecoxib-treated mice, AMD3100-treated mice, and EP3 KO mice were compared with those from vehicle-treated mice. Vehicle group; N=15. Celecoxib group; N=15. AMD3100 group; N=10. EP3 KO; N=5. Error bars indicate the mean \pm SE. $P < 0.0001$ (ANOVA). Student's t-test was used to evaluate significance differences at Days 3, 5 and 7 ($P < 0.05$).
- (G) SDF-1/CD11c double immunofluorescence staining of the subcapsular regions in regional lymph nodes 7 days after LLC implantation. Bar; 20 μ m. S; subcapsular regions, C; cortical regions.
- (H) Induction of SDF-1 in cultured DCs by stimulation with an EP3 agonist. DCs isolated from WT bone marrow were incubated with an EP3 agonist, ONO-AE-248 (0.01 nM), for 3 and 6 hours. The level of SDF-1 in the culture medium was determined with a specific ELISA. N=6. Error bars indicate the mean \pm SE. $P < 0.05$ (ANOVA). Student's t-test was used to evaluate significant differences at each time point ($P < 0.05$).
- (I) SDF-1 levels in cultured DCs isolated from the bone marrow of EP3 KO mice. The experimental conditions were the same as those in panel H. N=6. Error bars indicate the mean \pm SE. Statistical analysis was performed using ANOVA.

9-8. Figure 8. COX-2 derived PGE₂-EP3 signaling induces lymph node metastasis and lymphangiogenesis by facilitating DCs recruitment

- A) Recruitment of DCs intravenously-injected into the subcapsular regions of the regional lymph nodes. DCs were isolated from bone marrow cells derived from GFP transgenic WT mice and GFP transgenic EP3 KO mice. GFP-negative LLC cells were injected to the lungs of WT mice. Immunofluorescence images of SDF-1/GFP double positive cells in the regional lymph nodes were taken at Day 10. Bars; 100 μ m. S; subcapsular regions, C; cortical regions.
- B) Percentage of lymph node metastasis-positive mice receiving DCs from WT mice and EP3 KO mice. Injection of WT DCs facilitated lymph node metastasis, whereas injection of EP3 KO DCs did not. Vehicle; N=15. Other groups; N=5. $P=0.035$ (χ^2 test).
- C) CXCR4 immunofluorescence images (taken at Day 10) of the subcapsular regions of regional lymph nodes in WT mice receiving WT GFP-positive DCs. Many of the GFP-positive DCs were also CXCR4 positive. Bars; 20 μ m. S; subcapsular regions, C; cortical regions.

9-9. Figure 9. COX-2 derived PGE₂-EP3 signaling induces lymph node metastasis by facilitating the accumulation of Treg cells

- (A) Localization of Foxp3-positive cells in the subcapsular regions in regional lymph nodes 7 days after LLC injection. Vehicle, a typical result from vehicle-treated mice; AMD3100, a typical result from AMD3100-treated mice; EP3 KO, a typical result from EP3 KO mice. Bar; 50 μ m. S; subcapsular regions, C; cortical regions.
- (B) Temporal changes in the Foxp3-positive cell population in the regional lymph nodes after LLC injection. The results from celecoxib-treated mice, AMD3100-treated mice, and EP3 KO mice were compared with those from vehicle-treated mice. Vehicle group; N=15. Celecoxib group; N=15. AMD3100 group; N=10. EP3 KO; N=5. Error bars indicate the mean \pm SE. $P < 0.0001$ (ANOVA). Student's t-test was used to evaluate significant differences at Days 3, 5 and 7 ($P < 0.05$).
- (C) CD11c/TGF β 1 immunofluorescence images in regional lymph nodes from wild type mice and EP3 KO mice 10 days after LLC implantation. The number of CD11c/TGF β 1 double positive cells was markedly reduced in EP3 KO mice compared with that in WT mice. S; subcapsular regions, C; cortical regions. Bars; 50 μ m.
- (D) TGF β 1 secretion by WT DCs and EP3 KO DCs stimulated with an EP3 agonist (ONO-AE-248, 0.01nM). The amount of immunoreactive TGF β 1 in the culture medium was determined by ELISA. N=6. Error bars indicate the mean \pm SE. $P < 0.05$ (Student's t-test).
Temporal changes in TGF β 1 expression in the regional lymph nodes after LLC injection as determined by real time PCR. The results from celecoxib-treated mice, AMD3100-treated mice, and EP3 KO mice were compared with those from vehicle-treated mice. Vehicle group; N=15. Celecoxib group; N=15. AMD3100 group; N=10. EP3 KO; N=5. Error bars indicate the mean \pm SE. $P < 0.0001$

(ANOVA). $P < 0.05$ (Student's t-test).

9-10. Figure 10. COX-2 derived PGE₂-EP3 signaling induces lymphangiogenesis.

- (A, B, C) Temporal changes in the VEGF-C-positive cell population (A), the VEGF-D-positive cell population (B), and the VEGFR3-positive cell population (C) in the regional lymph nodes after LLC implantation. The results from vehicle-treated mice were compared with those from celecoxib-treated mice and EP3 KO mice. Vehicle group; N=15. Celecoxib group; N=15. EP3 KO; N=5. Error bars indicate the mean \pm SE. $P < 0.0001$ (ANOVA). Student's t-test was used to evaluate significant differences at Days 3, 5 and 7 ($P < 0.05$).
- (D) Immunofluorescence images of regional lymph nodes stained with the LYVE-1 antibody. Lymphangiogenesis was observed at the efferent side of the regional lymph nodes in vehicle-treated mice from Day 3, and was markedly reduced by celecoxib treatment. Bars; 100 μ m.
- (E) A schematic presentation of COX-2/SDF-1-dependent premetastatic niche formation. COX-2 and EP3 mediate the increase of SDF-1 at the premetastatic site prior to the arrival of tumor cells to the regional lymph node. CXCR4-positive tumor cells become mobilized to SDF-1 generating sites. Simultaneously, CXCR4/EP3-positive dendritic cells are recruited to generate SDF-1 in response to EP3 signaling.
- (F) Fate of metastasized LLC cells. Tregs are recruited to the premetastatic niche via SDF-1/EP3-signaling. The dendritic cells recruited to the premetastatic niche secrete TGF β 1 in an EP3/SDF-1-dependent manner. Thus, COX-2-PGE₂-EP3 signaling together with SDF-1/CXCR4 signaling may decide the fate of the colonizing LLC cells. Moreover, COX-2/EP3 signaling up-regulates lymph node lymphangiogenesis. Together, these events may facilitate tumor cell growth in the regional lymph nodes and lymph node or systemic metastasis.

10. Figures

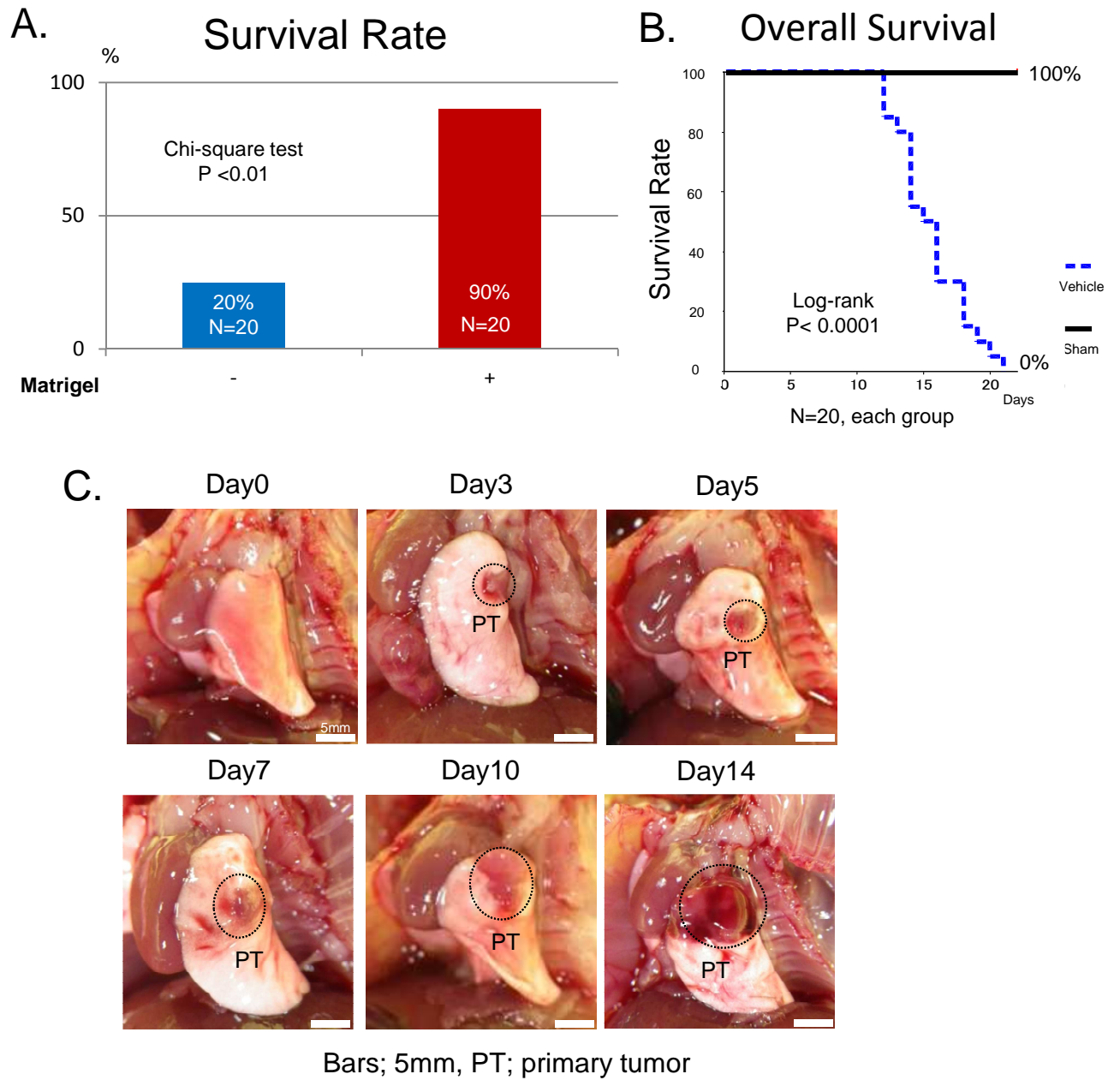
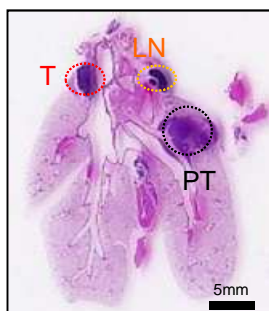


Figure 1

Vehicle (Day10)

A.



PT: primary tumor
LN: lymph node
T: Thymus

B.

Mediastinal lymph node metastasis

Vehicle	-	+	Rate
Day7	15	0	0%
Day10	10	5	33%
Day12	4	11	73%
Day14	1	14	93%

C.

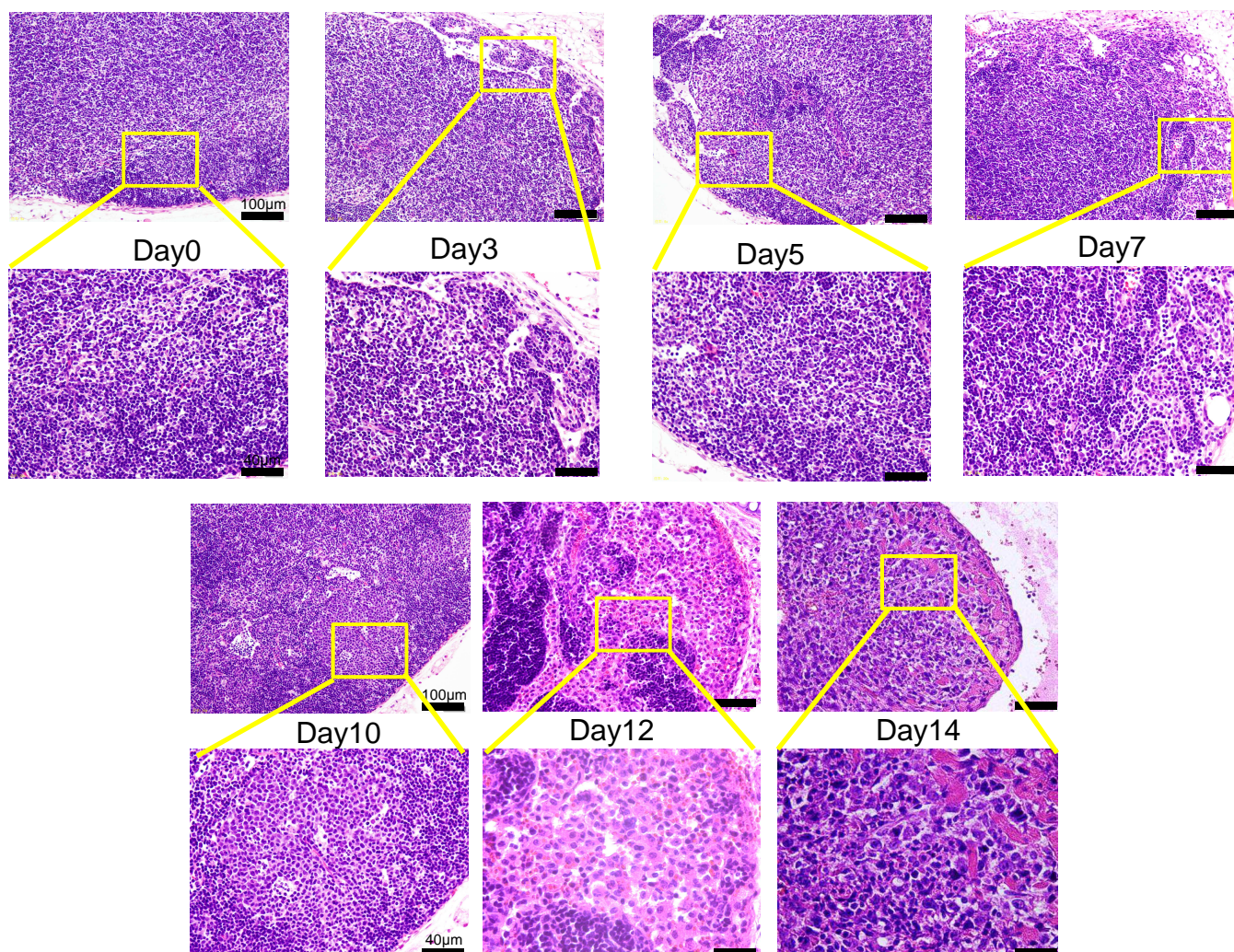
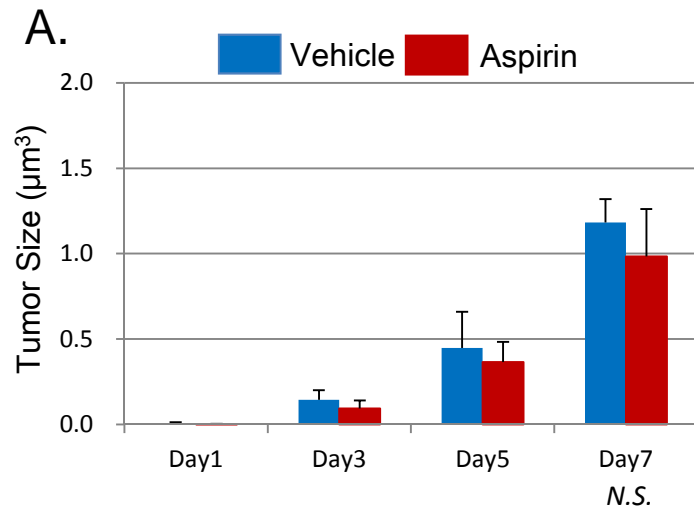
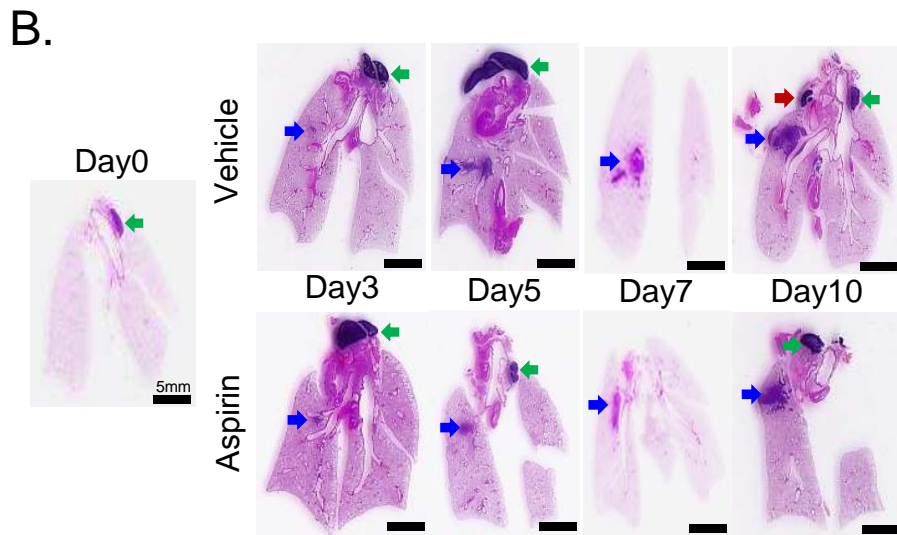


Figure 2



Error bars indicate the mean \pm S.E.



Bars; 5mm, blue arrow; primary tumor, red arrow; lymph node, green arrow; thymus

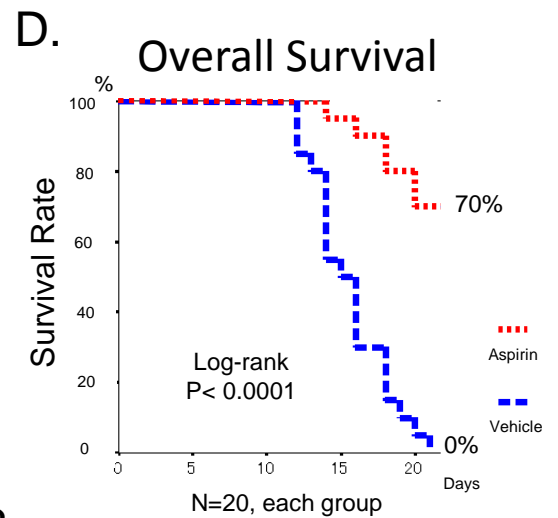
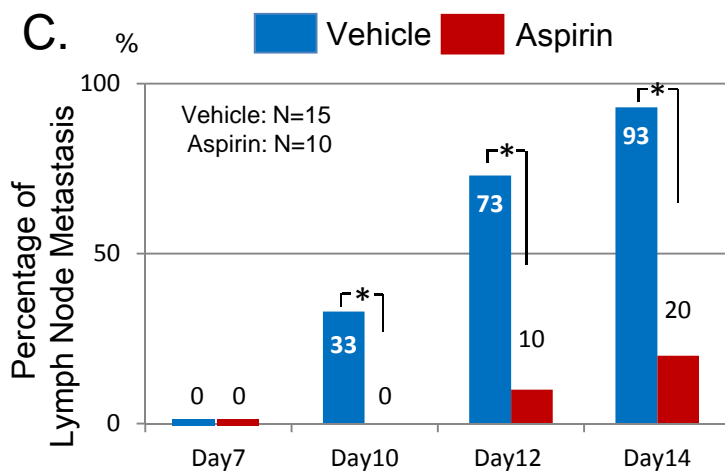


Figure 3

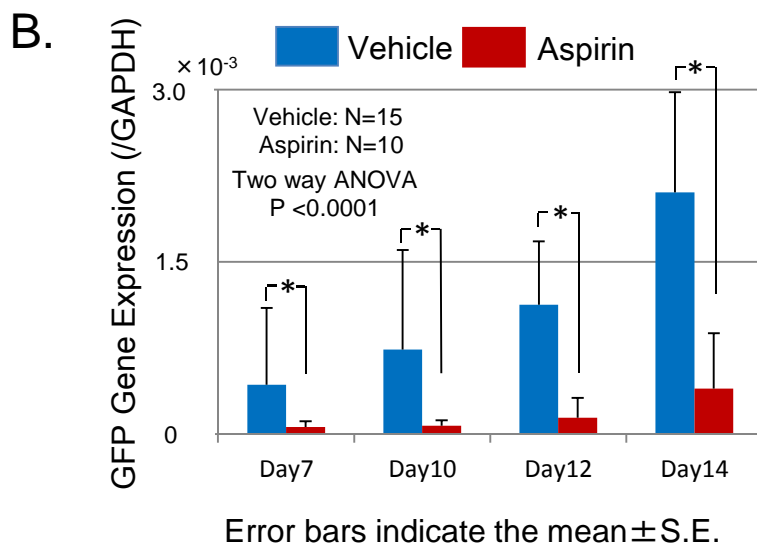
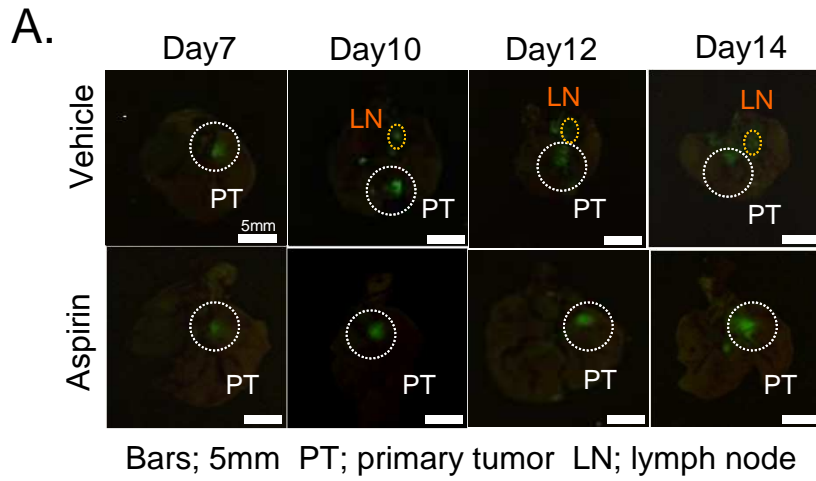


Figure 4

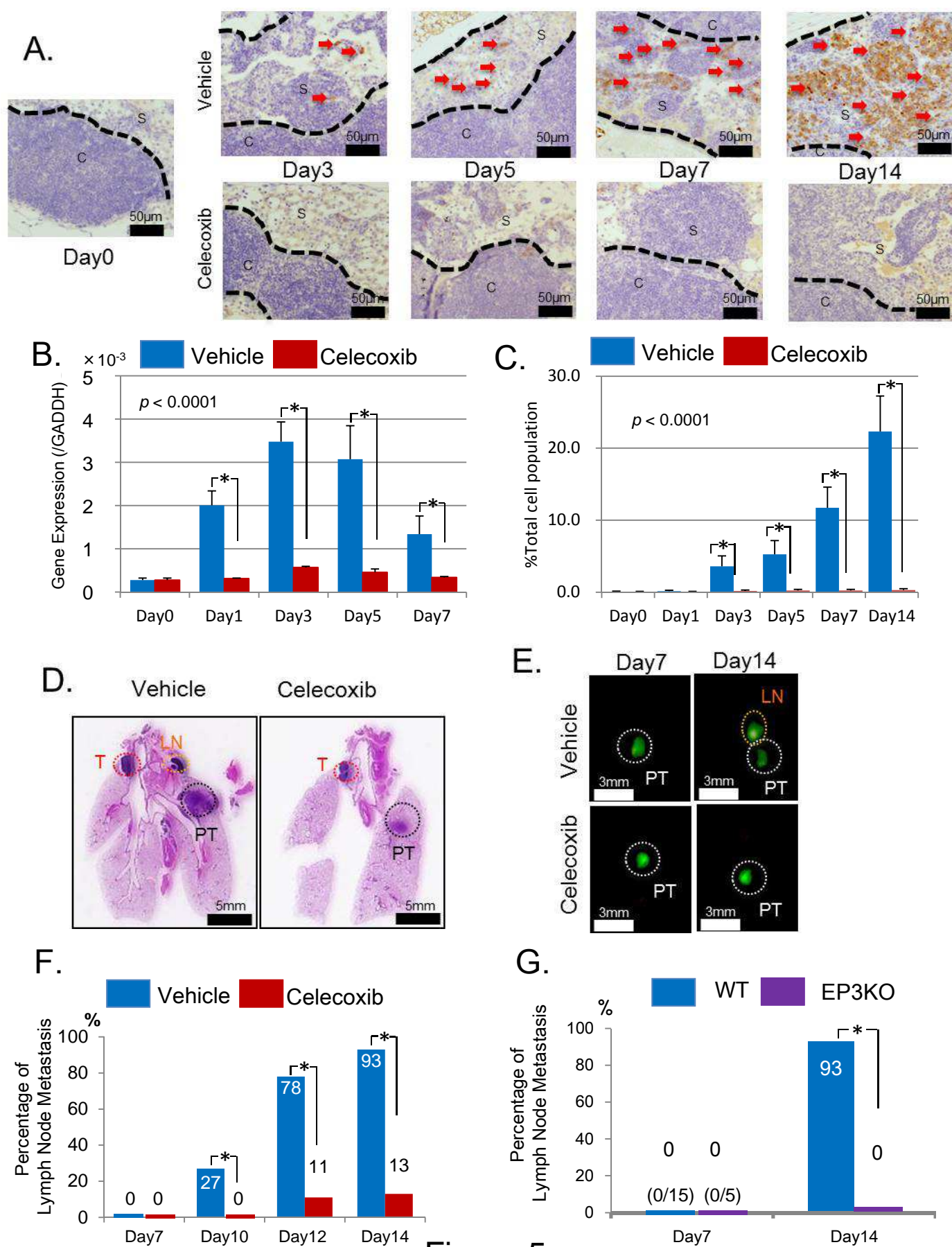


Figure 5

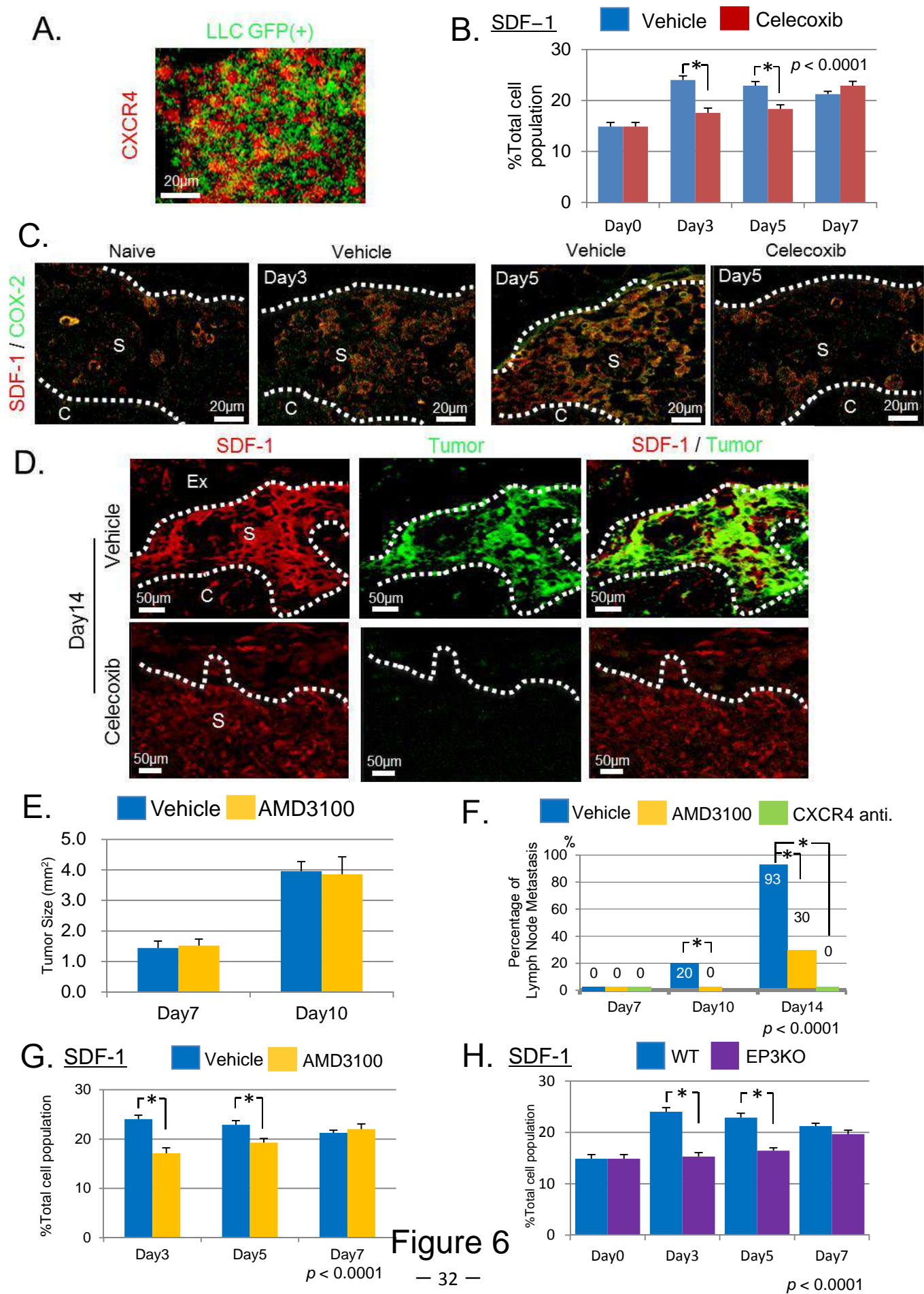


Figure 6

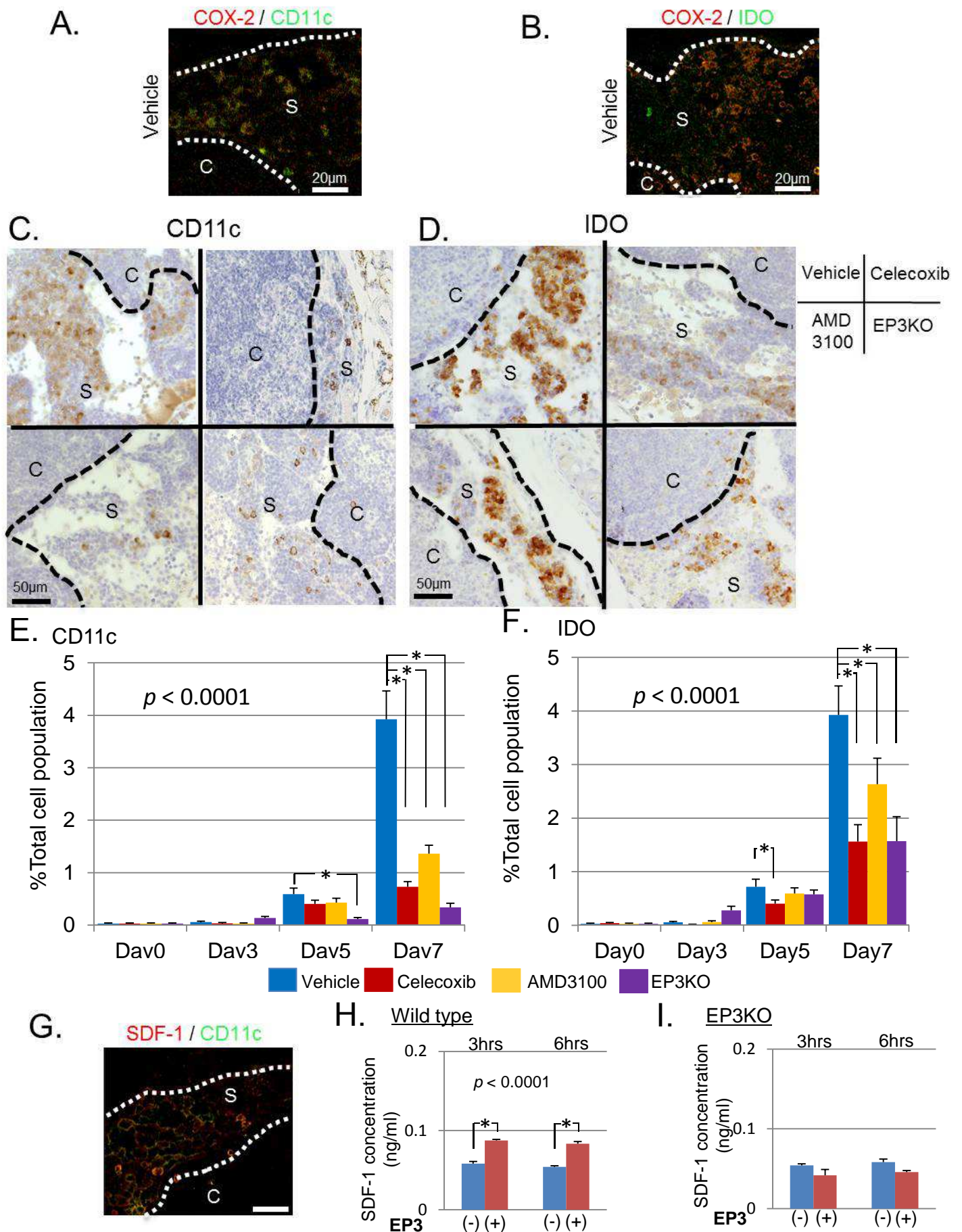
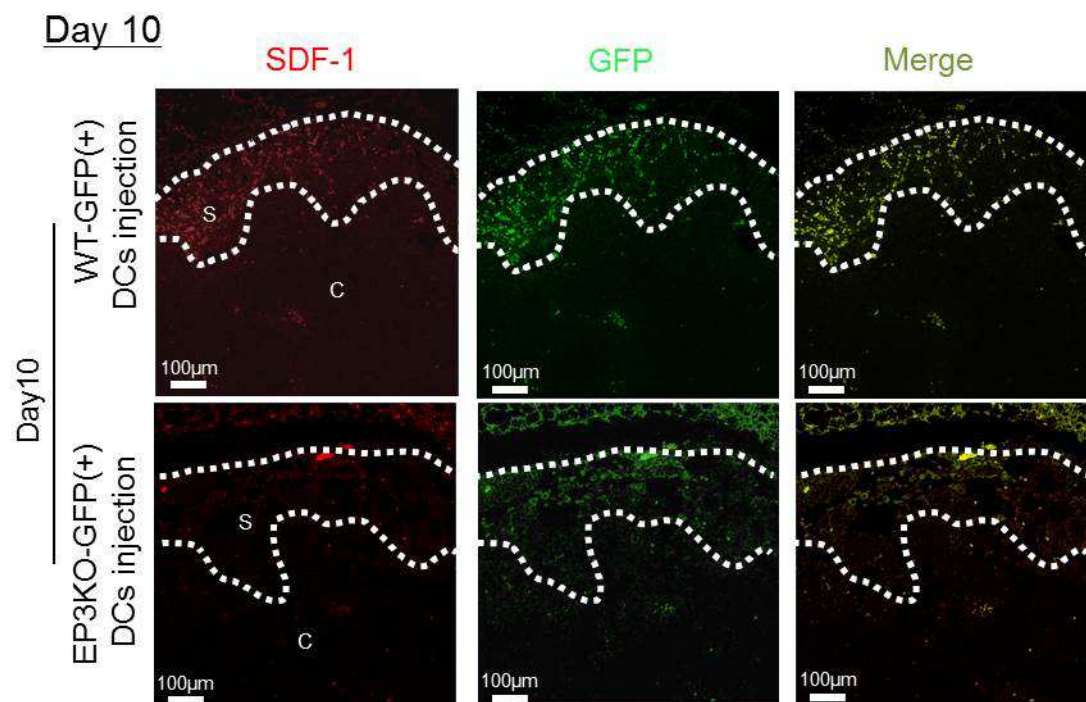
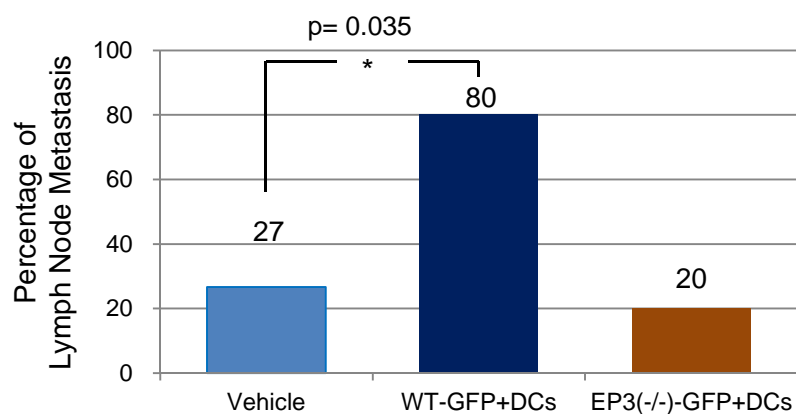


Figure 7

A.



B.



C. WT-GFP(+) DCs injection
Day 10

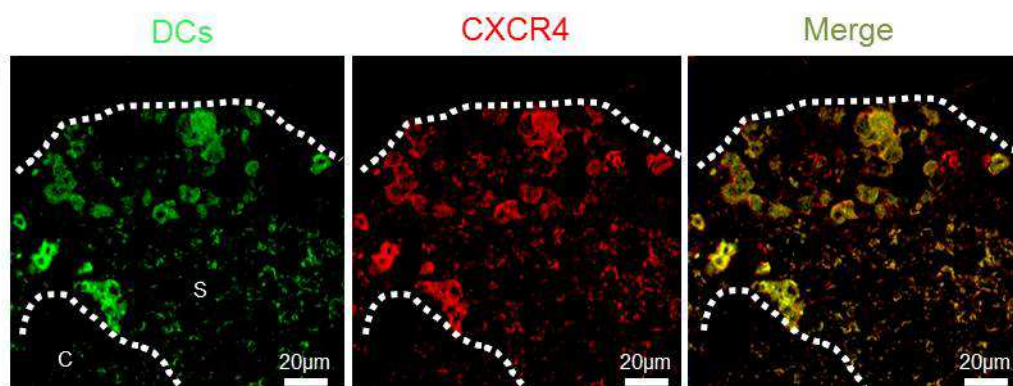


Figure 8

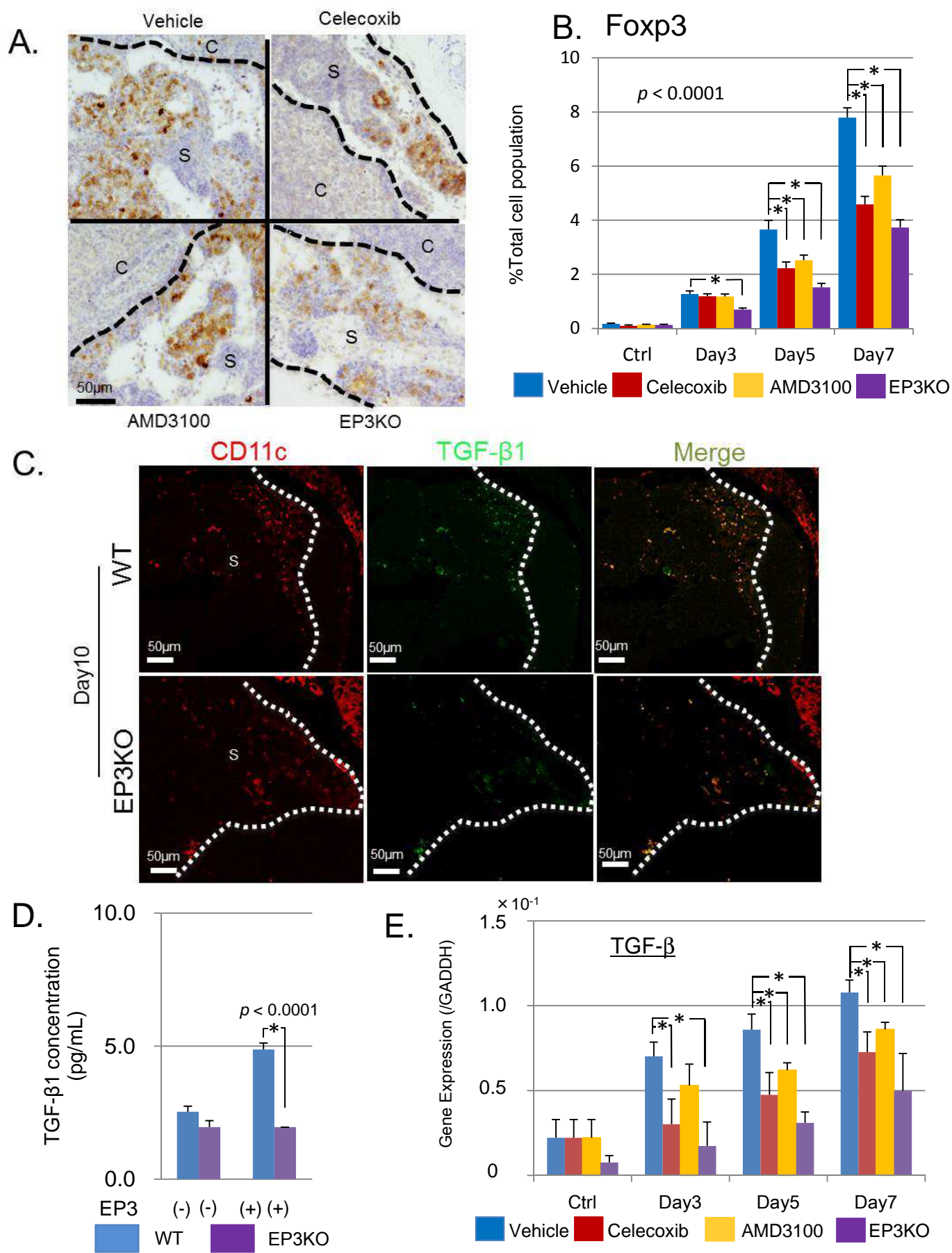


Figure 9

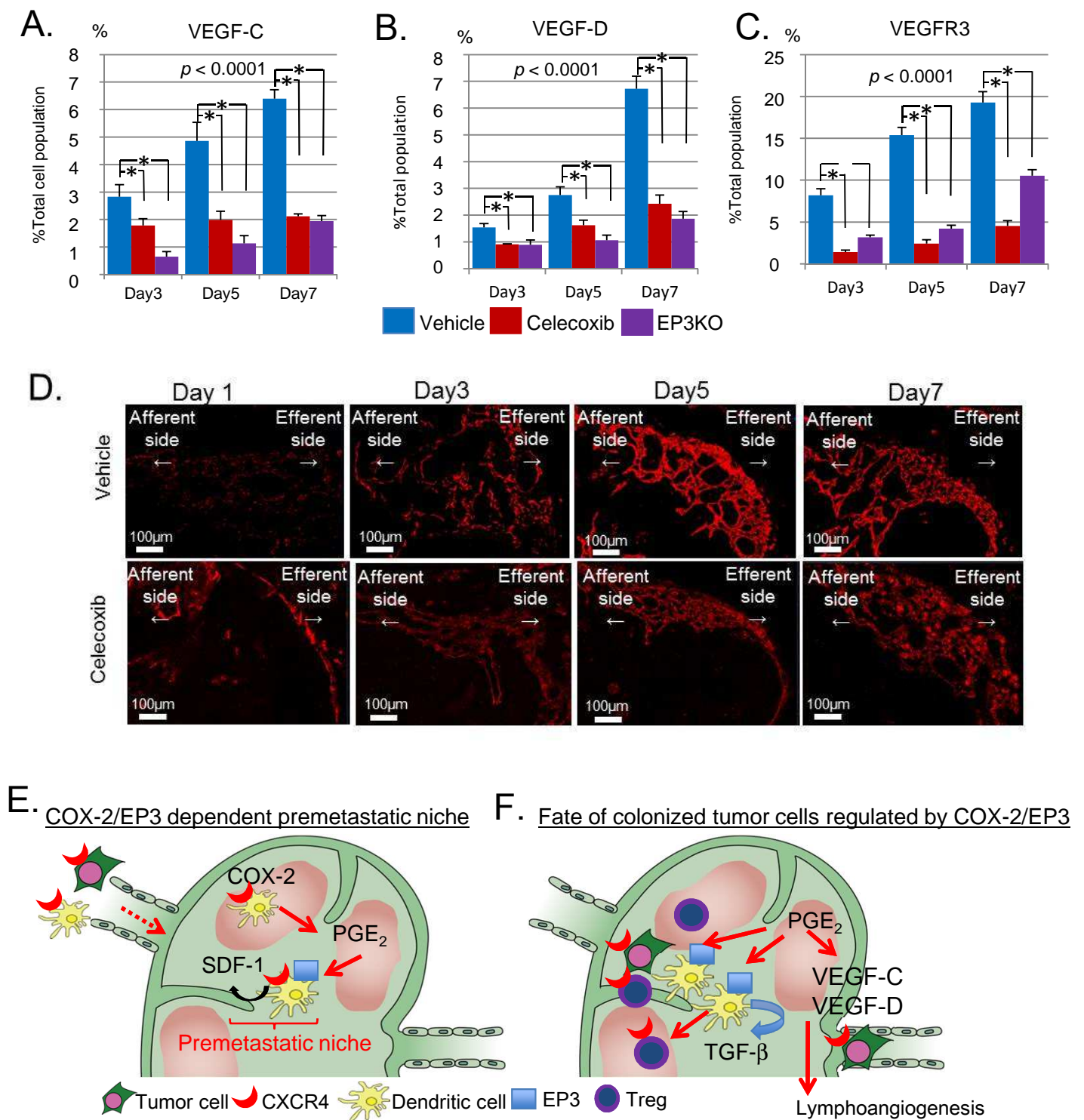


Figure 10

11. Supplemental Figures

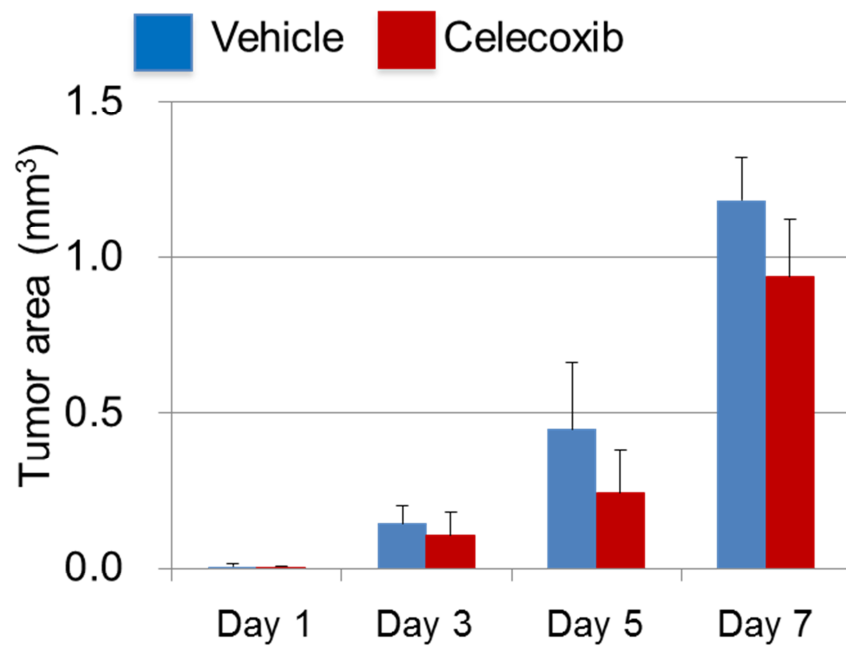


Figure S1. COX-2 inhibitor treatment does not affect the progression of the primary tumor in the early phase before regional lymph node metastasis.

Temporal changes in primary tumor growth after injection of LLC cells into the lungs. There was no significant difference (ANOVA) in primary tumor size between the vehicle- and celecoxib-treated group (100 mg/kg/day). Error bars indicate the mean \pm SE.

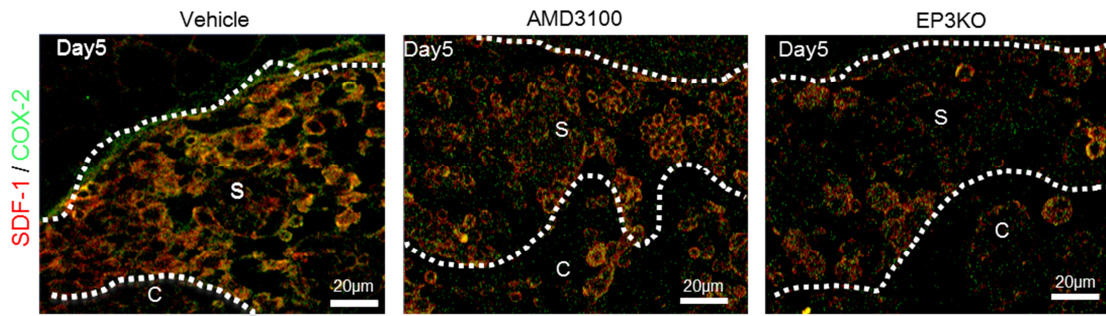


Figure S2. SDF-1 induction in regional lymph nodes is essential for premetastatic niche formation.

Immunofluorescence images of COX-2/SDF-1 expression in regional lymph nodes at Day 5 post-injection of LLC cells. COX-2/ SDF-1 double positive cells accumulated in the subcapsular regions at Day 5 before the arrival of GFP-negative LLC cells. AMD3100 treatment inhibited the accumulation of double positive cells. Accumulation of the double positive cells was reduced in EP3 KO mice compared with that in WT mice. Bars; 20µm. S; subcapsular regions, C; cortical regions.

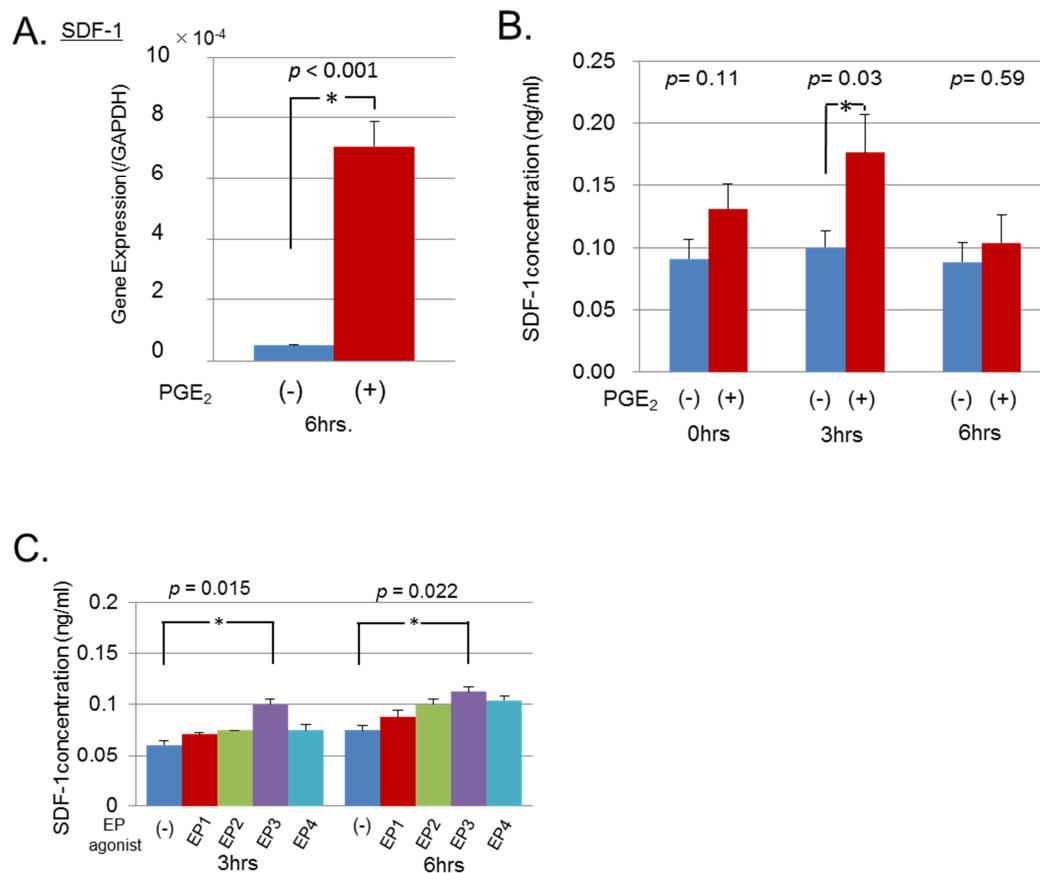


Figure S3. Effect of PGE₂ and EP agonists on the expression and secretion of SDF-1 in cultured DCs.

- (A) Addition of PGE₂ (0.01 nM) increased the expression of SDF-1 in cultured dendritic cells. Real time PCR was performed with SDF-1 primers as described in the supplemental methods. N=6. Error bars indicate the mean \pm SE. $P < 0.05$ (Student's t-test).
- (B) Time-course of SDF-1 secretion by cultured dendritic cells stimulated with PGE₂ (0.01 nM). The concentration of SDF-1 in the culture medium was determined by ELISA. N=6. Error bars indicate the mean \pm SE. $P < 0.05$ (Student's t-test).
- (C) Time-course of SDF-1 secretion by cultured dendritic cells stimulated with specific EP receptor agonists (0.01 nM). The concentration of SDF-1 in the culture medium was determined by ELISA. N=6. Error bars indicate the mean \pm SE. $P < 0.05$ (Student's t-test)

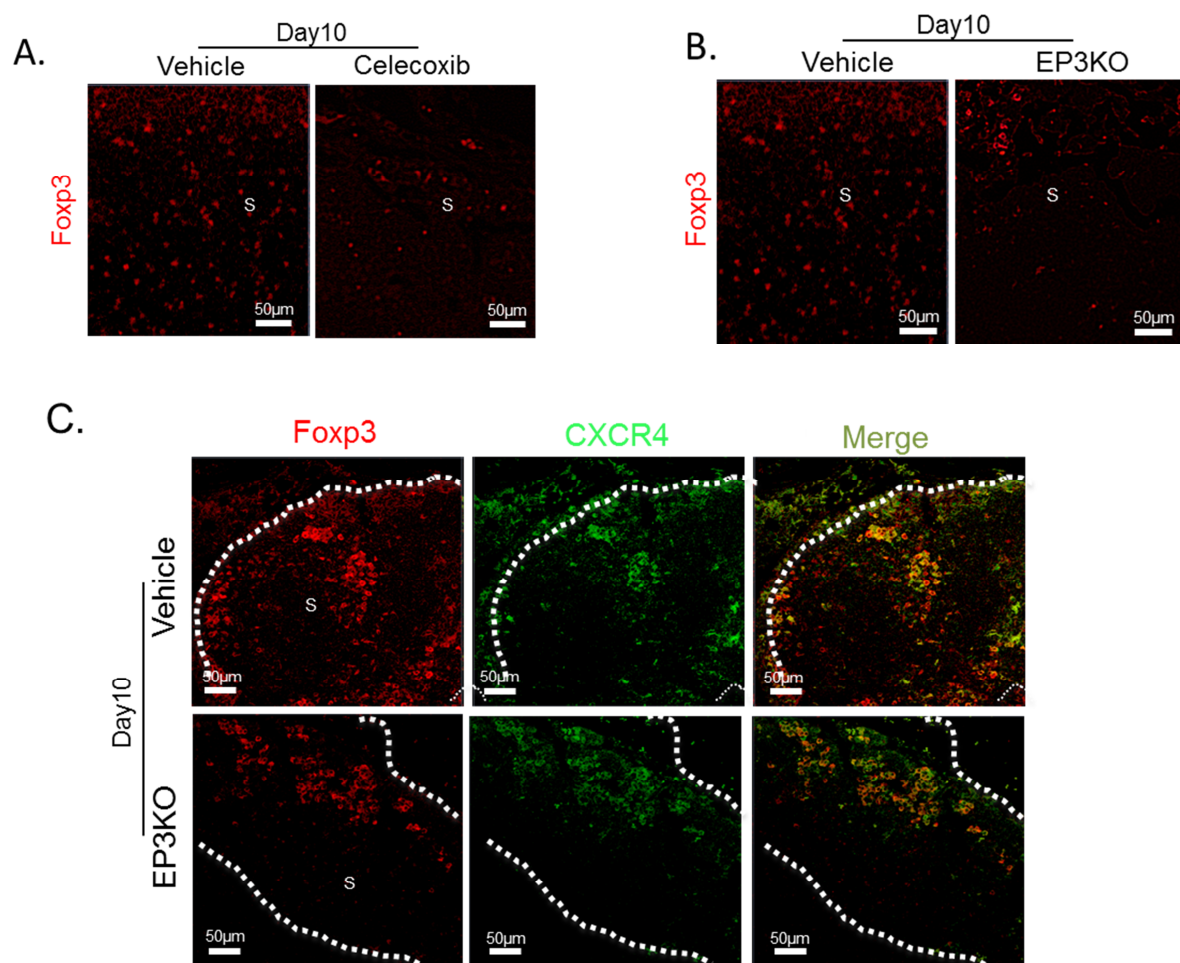


Figure S4. Regulation of Tregs induction by COX-2 derived PGE₂-EP3 signaling and effect on tumor metastasis

- (A) Immunofluorescence images showing Fxp3 in the subcapsular regions of regional lymph nodes at Day 10. Celecoxib treatment reduced the accumulation of Fxp3-positive cells. Bars; 50 μm. S; subcapsular regions.
- (B) Immunofluorescence images showing Fxp3 in the subcapsular regions of regional lymph nodes at Day 10. EP3 KO mice showed reduced accumulation of Fxp3-positive cells compared to WT mice. Bars; 50 μm. S; subcapsular regions.
- (C) Immunofluorescence images showing Fxp3/CXCR4 double positive cells in the regional lymph nodes after LLC injection at Day 10. The accumulation of Fxp3/CXCR4 double positive cells in the subcapsular regions was reduced in EP3 KO mice compared with that in WT mice. Bars; 50 μm. S; subcapsular regions.

12. Acknowledgement

I would like to express my special thanks to Prof. Masataka Majima and Dr. Hideki Amano for all advice and help and very thanks for Dr. Yoshiya Itoh, Prof. Hideroh Kitasato, Prof. Kazuya Iwabushi, Dr. Koji Eshima, Dr. Kayoko Hosono, Ms. Michiko Ogino, Ms. Mieko Hamano, and Ms. Kyoko Yoshikawa for many advices and their technical assistance. Finally, I would like to express my appereciation to Prof. Yukitoshi Satoh and my colleagues for giving me the opportunity to work the present study.